Biochimica et Biophysica Acta, 988 (1989) 351–376
Elsevier

BBAREV 85355

Hydration forces between phospholipid bilayers

R.P. Rand [1] and V.A. Parsegian [2]

[1] *Department of Biological Sciences, Brock University, St Catharines, Ontario (Canada) and* [2] *DCRT / NIDDK, National Institutes of Health, Bethesda, MD (U.S.A.)*

(Received 21 September 1988)

Contents

Abbreviations: *Polar groups:* PE, phosphatidylethanolamine; PC, phosphatidylcholine; PS, phosphatidylserine; DG, digalactosyl; MG, monogalactosyl, -Me, monomethylated; -$(Me)_2$, dimethylated. *Hydrocarbon chains:* DL, dilauryl; DM, dimyristoyl; DP, dipalmitoyl; DS, distearoyl; PO, palmitoyloleoyl; SO, stearoyloleoyl; DO, dioleoyl; DA, diarachinoyl; DD, didodecyl ether linked. *Particular lipids:* egg PC, PC extracted from hen eggs; egg PEt, PE produced by transphosphatidylating PE onto eggPC chains; Chol, cholesterol; PC-16-22, palmitoylarachinoylPC; DAG, diacylglycerol. *Other abbreviations:* SFA, surface force apparatus; OS, osmotic stress; PEO, alkylpoly(oxyethylene).

Correspondence: R.P. Rand, Department of Biological Sciences, Brock University, St. Catharines, Ontario, Canada L2S 3A1.

I. Introduction

In retrospect, perhaps, 'hydration forces' shouldn't have been surprising. After all, the defining principle of an amphiphile is to combine strongly polar and nonpolar drives within the same molecule. The phospholipids that mediate their hydrocarbon tails to create bilayers are faced with a phalanx of polar groups that must hold onto the solvent into which they would otherwise dissolve. The tenacity of holding this water, then, is part of a natural tension in amphipilic aggregates, a balance between the high energy of a hydrocarbon/water interface and the energy lowering adsorption of solvent. But why a force that extends ten or twenty ångströms and prevents the aggregates from making molecular contact? Most probes of water near bilayer surfaces indicate little perturbation beyond the first hydration layer. The answer appears to be in the very size of the membrane, the fact that the displacement of a bilayer entails the displacement of hundreds or thousands of water molecules. Even the tiniest energetic perturbation per water molecule is multiplied by hundreds or thousands to be an important energy on the scale of the bilayer membrane (Fig. 1).

So 'hydration forces', now known to dominate the interaction of most or all phospholipid membranes as they approach contact, remained unrecognized until relatively recent times. There were clear experimental signs, the restrained drainage of water from soap films independent of the ionic strength [1], the structural disjoining forces between polar surfaces [2–5] and the thickening of phospholipid bilayers resisting contact in multilayers undergoing dehydration [6–8]. But only during the past decade or so have these forces been systematically characterized in terms of their exponential decay, been compared with other operative forces such as van der Waals, electrostatic double layer and steric interactions, and been examined in terms of the molecular features of the bilayer surface that regulate them. Even now these interactions are just beginning to be utilized in analyses of membrane fusion and theories of phospholipid polymorphism.

This review comes at a time when phospholipid bilayer interactions are enjoying increasing attention from many laboratories. It is a time of healthy debate and careful examination of assumptions that go into various methods of measurement, a time when a great amount of data is being collected and many new questions are being posed before old questions are answered. We begin with a summary of various direct methods of force or energy measurement and then attempt to summarize the large body of experimental results in order then to allow comparison of material properties as well as methods of measurement. We next describe the ways in which hydration forces combine with other interactions occurring at 10–30 ångström separations and the ways these forces are expected to act in situations other than those in which they were measured, in phenomena such as in unilamellar vesicle interaction and bilayer phase transitions. In this way we hope to stimulate systematic work and further examination of outstanding questions relating these important forces to the microscopic properties of phospholipid assemblies.

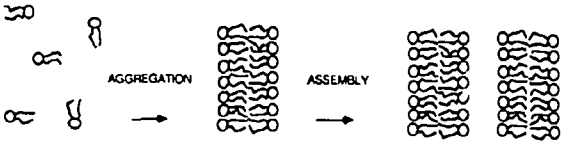

Fig. 1. The hierarchy of lipid aggregation and assembly into bilayers: the short-range driving force of hydrocarbon aggregation to form bilayers covered with polar groups; the assembly of bilayers into multilayer arrays whose spacing reflects long-range interlamellar forces

II. Measuring hydration repulsion

We will combine results from three complementary methods of force or energy measurement, osmotic stress, the surface force apparatus and pipette aspiration (Fig. 2).

Since each of these techniques provides direct measures of some quantities and is limited by inference of extrapolation for estimating others, the best strategy is to use all three to the extent possible. Apparent contradictions in results do occur, however, and their resolution can be instructive.

II-A. Osmotic stress (OS) method

The osmotic stress method of measuring interbilayer forces in multilamellar systems as well as between macromolecules in ordered assemblies has been reviewed recently in detail [12]. It is shown schematically in Fig. 2. The water in a multilayer array is brought to thermodynamic equilibrium with a second phase of known water activity. This equilibration can be achieved either by subjecting the multilayer to a polymer solution of osmotic pressure P whose large solutes cannot penetrate between bilayers; or the multilayer is physically squeezed under a pressure P in a chamber with a semi-permeable membrane to allow exchange with a reservoir of pure water; or the multilayer is brought to equilibrium with a vapor of known relative humidity (p/p_0) to create an effective osmotic pressure $(kT/v_w)\ln(p_0/p)$, where k = Boltzmann's constant, T is the absolute temperature and v_w the partial molar volume of water. The chemical potential of the water with which the lipid is equilibrated, whether varied osmotically, by mechanical means or through the vapor phase, gives the net repulsive pressure P between bilayers. X-ray diffraction of

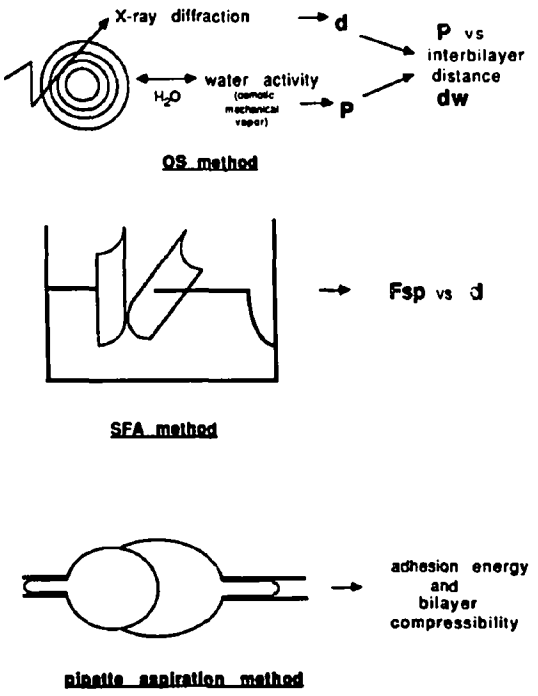

Fig. 2. Three ways of measuring forces between bilayers. Osmotic stress (OS) gives the dehydration or desolvation free energy of thermodynamically well-defined phospholipid phases equilibrated with water at different activities; the structural consequences of solvent removal are usually monitored by X-ray diffraction [9–12]. The surface force apparatus (SFA) is designed to measure attractive and repulsive interactions between crossed cylinders of mica coated with lipid bilayers and immersed in different solutions [13,14]. Pipette aspiration (PA) measures energies of adhesive contact between large unilamellar bilayer vesicles in solution, as well as bilayer strength or compressibility under lateral deformation [15–18].

that equilibrated phase gives the repeat distance d of the lipid plus water layers, often to better than ångström accuracy. The method is not limited to lamellar phases and has been applied recently also to inverted hexagonal phases, for example, see Ref. 19. The amount of water per lipid molecule, ΔV_w, removed under pressure P, yields the work of dehydration, $P\Delta V_w$, which is a change in the chemical free energy of the lipids. This work is independent of any model of hydration and of any assumptions about the structure of the phospholipid phase. Given the many ways of applying osmotic stress, it is possible to bring structures to virtually complete dehydration at pressures corresponding to over 1000 atmospheres, or $\log_{10} P > 9$ when pressures are measured in dynes/cm^2. Attractive forces cannot be measured directly, but are inferred from the point of balance between repulsive and attractive forces.

The assignment of a measured work of dehydration to a force or energy of interaction between bilayers or to a work of rearranging the bilayers requires dissection of the measured repeat distance d into a bilayer thickness d_l and separation d_w. It also requires recognition of the pressure P as both a lateral and an inter-bilayer stress [11].

If bilayers were incompressible, then changes in repeat spacing d would equal changes in bilayer separation d_w. A force vs. distance relation could automatically be constructed from measured pressure P vs. repeat spacing d reduced by a constant bilayer thickness d_l. But bilayers are laterally compressible [15,20–23]. The same isotropic osmotic stress that pushes bilayers together also acts to deform them laterally [11,24]. There is a predicted decrease in cross-sectional area A and bilayer thickness d_l. Consequently, estimates of these structural changes are required in order to estimate bilayer separation d_w (Fig. 3).

In the Appendix we describe more fully three ways of gauging the bilayer thickness but they are summarized as follows.

First, the gravimetric traditional procedure of Luzzati divides the repeat spacing d into a lipid layer thickness d_l that contains all the lipid and none of the water plus a water layer d_w that contains only water [6]. This division requires a knowledge of specific volumes of the lipid molecules and their parts and of the intervening water. A compendium of these is given in the Appendix. The procedure is to measure repeat spacing d as a function of the known lipid/water ratios in gravimetrically prepared samples. As long as the repeat spacing d is monotonically increasing with the volume of water V_w per lipid molecule, one can convert the d spacing obtained under osmotic stress into a bilayer separation d_w for that d spacing in the gravimetrically prepared sample. The procedure works well except near limiting, or saturating, amounts of water where slight changes in d with added water make an accurate determination of water content difficult. While this approach provides clear evidence of bilayer deformation, it circumvents the difficult issue of interfacial structure.

Second, the 'electron density' profile determined from low-resolution X-ray diffraction analysis can be used as an estimate of bilayer thickness. A comparative study [25] showed differences between thicknesses measured this way and by the gravimetric method. Similar differences have been found by others [26]. In an analysis of 15 ångström resolution electron density maps as a function of osmotic stress, McIntosh and Simon [27] have concluded that that there is essentially negligible bilayer deformation. However, low resolution requires assumptions about the structure of the interface and that the bilayer thickness should be taken as the distance between two electron density maxima corresponding to the center of the polar groups plus a 5 ångström width on each side of the bilayer to include the (hydrated) headgroup. Their estimates of hydration energy refer then to dehydration to the point of outermost

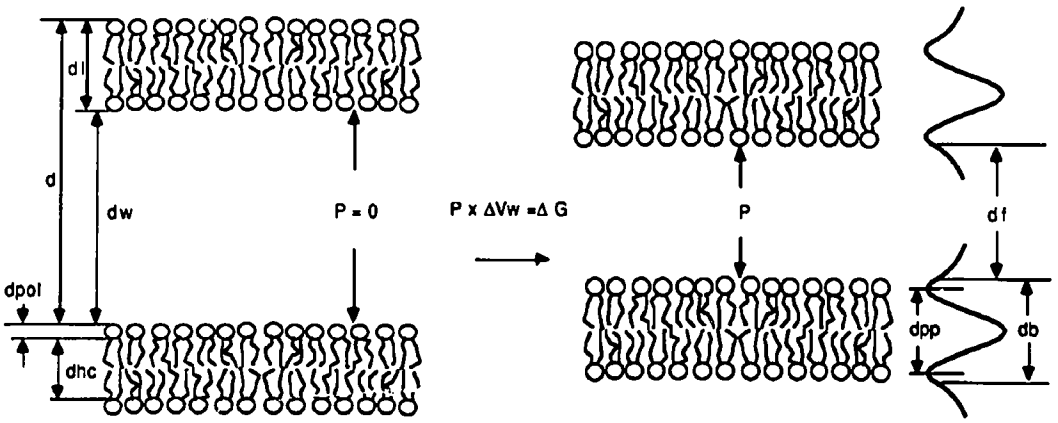

Fig. 3. Geometric parameters for describing bilayer thickness and separation as a function of applied pressure. The repeat spacing d is traditionally divided into a pure lipid layer of thickness d_l and a pure water layer thickness d_w. The volume of water per lipid molecule can be written as $V_w = A \cdot d_w/2$ where A is a mean cross-sectional area projected onto the average plane of the bilayer. A further division of d_l is to imagine a pure hydrocarbon interior of thickness, d_{hc}, between two polar layers, d_{pol}, that contain the lipid polar groups. The work of removal of water ΔV_w under applied pressure P is a change $P\Delta V_w = \Delta G$ in the lipid bilayer free energy. Such pressures cause decrease in area A as well as in separation d_w. It is sometimes possible to describe the bilayer dimension by low resolution electron density distributions whose peaks correspond roughly to the location of the lipid-water interfaces. The peak-to-peak distance d_{pp} plus a constant to include the width of the polar group layer is defined to be a layer thickness d_b. The remaining space, d_f ($= d - d_b$) is another measure of separation.

contact between these bilayers. The decay distances from this method are understandably different from those which envisage bilayer deformation. Furthermore, conclusions about relative bilayer separations among lipids can depend on which method of determining separation is chosen (see Appendix). Ultimately, the estimated work needed to push bilayers to 'contact' will depend dramatically on the convention used to define the 'zero' of separation.

Third, by the 'compressibility' method [36] one can use independently measured bilayer compressibilities. Each of the above approaches suffers from being only an insensitive measure of bilayer compressibility, i.e., a measure of the changes in bilayer thickness or molecular area with changes in hydration. However, this difficulty can be circumvented by using the recent independent, very sensitive measurements of bilayer compressibility itself [18]. One may begin by using either the gravimetric estimates of d_l and d_w at low enough hydration to be quite accurate, or the estimates from electron densities. Then, using measured lateral compressibilities it is possible to compute bilayer deformation and changes in d_l and d_w over a range of deformation for which compressibility is known. We now consider this procedure, which replaces the weakest step in earlier methods with a precise measure of required quantities, to be the best way now available to determine the variation of bilayer thickness with separation and hydration. The empirical P vs. d_w fits given in Table I use this procedure, originally suggested to us by E. Evans (personal communication). This 'compressibility' approach neatly reconciles data originally interpreted either by the 'gravimetric' or 'electron density' analyses, giving identical dehydration energies and pressure decay rates as functions of bilayer separation.

Extracting hydration pressure, P_h, from P. Dissection of the measured net pressure P into its physically distinct components is a problem almost as difficult as the theoretical explanation of those components themselves. For convenience, we imagine that the net force per unit area is made up of three kinds of interactions: P_h due to surface hydration, P_{vdw} from (attractive) van der Waals or dispersion forces, and P_n from the structural fluctuations of the thermally excited bilayers. Since a proper theoretical formulation of any of these components poses severe problems at the observed distances of bilayer encounter [36], we emphasize here an empirical description of P vs. d_w rather than force the data to fit into an arbitrary formalism. Still, some assumptions must be made.

Except near the limit of swelling in unlimited amounts of water, the nature of the force observed between neutral bilayers is essentially exponential with decay distance λ of some 1–3 ångströms. We therefore describe this force in the form

$$P_0 \exp(-d_w/\lambda)$$

by fitting to points that are well away from the region where attractive forces create a deviation from exponential.

II-B. Surface force apparatus

A second method of force measurement, recently applied to phospholipid bilayer interactions, is by means of a 'surface force apparatus' (SFA) [13,14]. Here, one

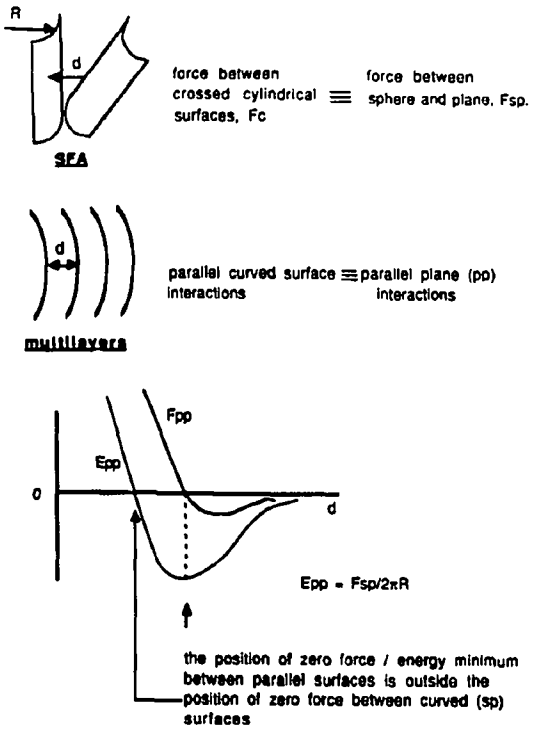

Fig. 4. Forces between crossed cylinders compared to those between parallel surfaces of the same material. By the Derjaguin approximation, the force between crossed cylinders F_c is equivalent to that between a sphere and plane F_{sp}; it corresponds to the energy E_{pp} between parallel surfaces when their separation, d, is much less than the radius of curvature R. The relation between them is $E_{pp} = F_{sp}/2\pi R$. The separation at the point of force balance (or minimum energy) between long-range attraction and shorter range repulsion will always occur at smaller separations for oppositely curved surfaces than for parallel surfaces. Remarkably, the equilibrium separation between oppositely curved surfaces is independent of their size.

coats lipids, either by adsorption from suspension [28] or by passage through monolayers [29] onto mica sheets glued down onto cylindrical surfaces. One measures the distance between the crossed cylinders by means of interference fringes that are set up between the silvered backs of the mica sheets. Forces between the surfaces of the crossed cylinders are read from the deflection of a cantilever spring system of variable tension that can be moved to bring the surfaces to a given separation. Repulsive forces are seen as a continuous deflection away from contact and are limited only by the onset of deformation of the mica surface. Attractive forces are seen either from the position of a jump into 'contact' as surfaces are brought together with springs of different thickness, or from the position of a jump away from a spontaneously assumed minimum energy position. Relative changes in position can be measured to accuracy of 1 ångström. The 'zero' of separation is computed by subtracting from the measured distance of contact between half-bilayers in air and subtracting again the thickness of a bilayer based on the estimated phospholipid volume and the lipid cross-sectional area of the source monolayer.

Two important differences between this method and applying osmotic stress to spontaneously forming multilayers are (1) the immobilization of the bilayers that comes from attachment to the mica surface and (2) the cylindrical versus parallel geometry. To correct for the geometry, the mica surface measurements routinely assume the validity of a transformation, according to Derjaguin [30] the force between crossed cylinders of equal radius R is the same as the force, F_{sp}, between a sphere of radius R and a plane flat surface. Further, this *force* F_{sp} is equivalent to the *energy* E_{pp} between plane parallel surfaces of the same material. Specifically,

$$E_{pp} = F_{sp}/2\pi R$$

For this reason, forces F_{sp} measured with the SFA are routinely plotted as F_{sp}/R and are therefore implicitly related to the *Energy* rather than the *Force* between parallel surfaces.

The position of a spontaneously assumed minimum energy (zero force) position between bilayers in the multilayer system will occur at a greater separation than that seen as a point of force balance in the mica cylinder system (see Fig. 4). So, to compare forces measured on multilayers with those between crossed cylinders it is necessary either to differentiate the cylinder-cylinder forces or to integrate multilayer forces from a hypothetical infinity [32].

The observation [31] that mica surfaces will bend at $F_{sp}/R \approx 10$ dyne/cm allows one to estimate an upper limit on the equivalent pressure between planar surfaces to which the SFA method can be used. We can say that an exponential pressure P of decay rate λ corresponds to an energy, $\lambda P = E_{pp}$ with a maximum value $\approx 10/2\pi \approx$ dyne/cm. Then for $\lambda \approx 2$ Å, typical of phospholipid hydration repulsion, the maximum pressure will be $P \approx 10^8$ dyne/cm^2.

Given all these differences in technique it is pleasing to see the good agreement between estimates of hydration forces from the two techniques [32] as will be described below.

II-C. Pipette aspiration

Evans [15–18] has developed a procedure, schematically shown in Fig. 2, for manipulating vesicles aspirated into the ends of pipettes in order to determine mechanical properties of isolated vesicles and contact energies of adhering vesicles. On an isolated vesicle, one measures the tongue length inside the pipette as a function of applied suction pressure ΔP. At first, small pressures

have a large effect on the tongue length, because of the removal of bends and folds; then the bilayer becomes taut with the subsequent length/pressure relation reflecting the bilayer area elasticity. We follow Evans' terminology in referring to the modulus of this elasticity as a 'compressibility'.

For bilayer adhesion measurements, two vesicles are drawn taut and brought to contact on the ends of approximately coaxial pipettes. Measured diameters and tongue lengths are used to determine bilayer area. Then, keeping both pipettes fixed and maintaining tension on one vesicle, tension is relaxed on the other allowing it to spread over its taut neighbor. Measurement of the diameter of the contact area together with monitored pressure and tongue length allows determination of contact angle and lateral tension in the bilayer. These then combine using Young's equation to give the adhesive contact energy, G_{min}, as described below. These are used as a standard to compare with energies derived from the integrated force curves from the osmotic and SFA techniques.

III. Maximum hydration and structural dimensions of lipid multilayers

The most unassuming measure of the strength of hydration of bilayers is the amount of water multibilayers imbibe from excess solution. Whether determined from the simpler gravimetric method or further refined by adjusting for compressibility makes little difference to the measured volume of water per lipid molecule (compare Tables I and VII). Polar group identify, polar group methylation, the physical state of the hydrocarbon chain, chain heterogeneity and mixing of lipid species, all appear to affect total hydration. We have grouped the entries in Table I to facilitate recognition of these factors without intending to obfuscate other comparisons that might occur to the reader. This is not a comprehensive list of lipids that have been studied, but is culled from the more recent of an extensive literature of phospholipid phase diagrams selected to highlight the major differences in maximum hydration of neutral lipids or charged lipids in high ionic strength. Also we have used the preferred compressibility-adjusted values where available, otherwise the gravimetric values. Still, it is worth noting that there is little difference between qualitative comparisons using the gravimetric and those using compressibility derivations. This updates an earlier review of phospholipid hydration [33].

In order to make comparisons among lipids which differ in the size of their polar group, the maximum volume of water per molecule, V_{wo}, has been normalized to V_{wo}/PE, a volume of water per polar group mass equal to that of PE. One will note that differences in the amount of water usually correlate with comparable differences in maximum bilayer separation in excess water d_{wo}.

The most striking factor that increases maximum hydration is methylation of the polar group layer. This is summarized in Fig. 5 where maximum hydration V_{wo}/PE is plotted as it varies with the number of methyl groups per 100 Å^2 of polar group surface. The dramatic effect of methylation is seen among the following factors which affect maximum hydration.

Hydration of lipids with different polar groups. In the comparisons of the homogeneous synthetic lipid the PEs, DOPS, SOPC and DGDAG, the methylated species hydrate nearly twice as much as the other lipids. As a class, phosphatidylcholines (PCs) hydrate more than PEs even though there is a wide range of sorption within each class. Compare, for example, palmitoyloleoylPE (POPE) with stearoyloleoylPC (SOPC) whose hydrocarbon chains differ by only a -CH_2-CH_2- link in one chain. Their cross-sectional areas A_0 differ by less than 15%, bilayer thickness d_{lc} by less than 3%, yet the volumes taken up and bilayer separations differ by more than a factor of two.

Dioleoylphosphatidylserine (DOPS), a charged lipid, put in 0.8 M NaCl to screen out electrostatic repulsion, and digalactosyldiacylglycerol (DGDAG), a neutral species, swell only as much as POPE. However, the swelling of melted chain PCs, egg and dilauryl at room temperature, dimyristoyl at 27°C and dipalmitoyl at 50°C, are much like SOPC. To us the higher hydration suggests the action of polar group methylation, the defining difference between the PCs and their unmethylated sisters.

Polar group methylation. In the methylation of egg PEt to egg PC, large but disproportionate increases in hydration results with each methylation. Beginning with egg PEt, a PE created by replacement of the polar groups of egg pC, then creating singly (egg PEt-Me) and doubly (egg PEt-Me_2) methylated derivatives, one may systematically examine the effect of methylation alone. A single methylation results in a 28% increase in hydration, while successive methylations give 7% then 16% increases for the fully methylated PC. This is also seen with the successive methylations of DOPE [39] and DMPE (not shown in Table I) [40]. (see also Refs. 46 and 47.)

Methylated lipids added to bilayers. These last effects of methylation hold also when the methylation of the polar layer is varied by mixing, in the bilayer, methylated and unmethylated species, either SOPC and POPE, shown here, or egg PC and egg PE [41]. Fig. 5 shows a remarkable parallel between these mixed bilayers and the methylated series just described.

These studies of the systematic methylation of bilayers show that there is a disproportionate effect of the first methyl groups. A single methylation of the PE polar group results in a large increase in hydration, with

TABLE I

Parameters

Repeat spacings of lamellar lattices in excess water, d_0, are directly measured. Water content expressed as dry weight fraction, c_0, cross-sectional areas, A_0, and bilayer separation, d_{wo}, again in excess water, are derived either by the gravimetric method or, where osmotic stress data have been measured, by the new 'compressibility' method (see text and Appendix) using the compressibility K (dyne/cm) either directly measured or inferred. Volume of water per lipid molecule $V_{wo} = A_0 d_{wo}/2$. For comparison among different species, this volume has been renormalized as V_{wo}/PE, the volume of water per mass of PE headgroup. Hydration force parameters, P_0 and λ, are fitted to data in the high pressure region where log P vs. separation is a straight line. The G_{min} (erg/cm^2) are absolute values of negative quantities; these estimates are based on extrapolation of exponentially decaying P to separation d_{wo} with the assumption of a van der Waals attraction vs. exponential hydration repulsion. Data without a reference number are our unpublished results.

	d_o (Å)	c_o	A_0 (Å^2)	d_{lo} (Å)	d_{wo} (Å)	V_{wo} (Å^3)	V_{wo}/PE (Å^3)	K (dyne/cm^2)	λ (Å)	log P_0 (dyne/cm^2)	G_{min} erg/cm^2)	Ref.
DDPE	45.8	0.72	55	32.5	13.3	365	365					34
DAPE	57.3	0.79	58	47.3	10	290	290					34
DLPE	46.1					270	270					35
POPE (30 °C)	53.2	0.79	56.6	41.8	11.4	323	323	233	0.8	12.5	0.14	36
DOPS (0.8 M)	53.5	0.74	70	39.6	13.9	485	361					
SOPC (30 °C)	64.6	0.63	64.3	40.6	24	771	667	200	2.0	10.5	0.02	36
DGDG	53.2	0.73	79.8	38.8	14.4	574	328	200	1.7	10.3	0.24	37
POPE/SOPC												
19/1	54.5											36
9/1	56.4	0.74	57.3	41.7	14.7	421	415	233	1.3	11.2	0.09	36
4/1	59.5											36
2/1	61.2	0.68	58.5	41.5	19.7	576	559	222	2.1	10.0	0.08	36
3/2	63.3											36
1/1	63.8											36
DGDG/SOPC												
45/55	57.2	0.68	72.8	38.9	18.3	666	467	200	1.8	10.6	0.18	
DGDG/POPE												
1/1	54	0.72	70.2	38.9	15.1	530	385	216	1.7	10.3	0.23	
DOPE/DOPC												
3/1	58	0.67	63.8	38.6	19.4	619	597	200	1.8	10.2	0.03	
eggPE	52.9	0.64	72.1	33.8	19.1	690	690	200	1.3	12.5	0.14	38
DOPE (−2°C)	52	0.70	65	37	15	487	487					39
DOPE-Me (−2°C)	61	0.63	62	39	22	682	648					39
DOPE-(Me)$_2$ (−2°C)	62	0.60	66	38	25	825	747					39
DOPC (−2°C)	61	0.59	70	36	24	840	727					39
eggPEt	52	0.72	65	37.4	14.6	474	474	200	1.1	12.3	0.20	36
eggPEt-Me	61.8	0.66	60.7	40.8	21	637	605	200	1.8	10.3	0.01	36
eggPEt-(Me)$_2$	63.1	0.64	62.6	40.4	22.7	713	646	200	1.8	10.4	0.01	36
eggPC	61.9	0.60	69.5	37	24.9	866	749	145	2.1	10.6	0.03	36
PC 16-22	63.5	0.60	69.3	38.3	25.2	873	758	145	2.1	10.1	0.01	
eggPC/CHOL 1/1	65.5	0.64	95.6	42	23.5	1126	929	1000	1.1	13.8	0.003	38
DPPC/CHOL 1/1	66	0.65	87.9	43.1	22.9	1005	872	600	1.5	11.5	0.01	38
eggPC/DAG-12.5	63	0.58	81.2	36.6	26.4	1070	829	145	2.4	10.4	0.05	42
DLPC	59	0.54	64	31.6	27.4	877	761	145	2.0	10.6	0.01	38
DMPC (27 °C)	62.2	0.57	61.7	35.7	26.5	816	708	145	2.2	10.5	0.02	38
DPPC (50 °C)	67	0.54	68.1	35.9	31.1	1059	919	145	2.1	11	0.01	38
DOPC	64	0.56	72.1	35.9	28.1	1013	862	145	2.1	10.6	0.01	38
DPPC (25 °C)	63.8	0.74	48.6	47.1	16.7	405	351	1000	1.2	12.3	0.03	38
DSPC	67.3	0.71	51.6	47.7	19.6	506	431	1000	1.3	12.9	0.15	38
DPPC/Chol 8/1	80	0.64	47.5	50.8	29.2	694	602	1000	2.0	10.7	0.004	38

smaller increases on successive methylations. SOPC/POPE mixtures 2/3 hydrate to the same extent as pure SOPC. These disportionate effects suggest that beyond bringing their complement of water to these mixtures, lipids with methyl groups induce a structural change in PE bilayers that result in further hydration.

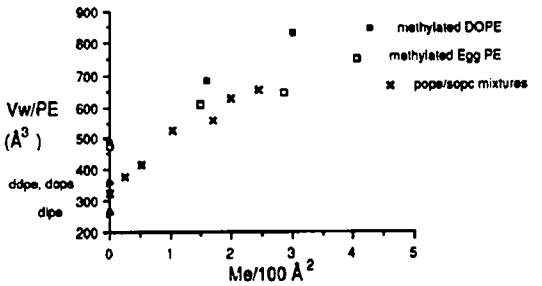

Fig. 5. The uptake of water by multilayers under zero osmotic stress correlates strongly with the density of polar surface methyl groups. The correlation seems to hold whether methyls are successively bound to polar groups (squares) or are added by mixing methylated (SOPC) and unmethylated (POPE) species (X symbols). Pure DDPE and DLPE, as well as a non-methylated DOPS in solutions of high salt concentration, hydrate in the same low range as DOPE and POPE. DOPE data from Ref. 39, POPE data from Ref. 34 the data for the remainder are from Ref. 36.

We suggest later in the text that this change is a disruption of hydrogen bonding that appears as an attractive force between (PE) bilayers [36].

Chain melting and heterogeneity. There are differences in hydration that appear to reflect effects of the hydrocarbon chains. Gel phase lipids hydrate less than their melted counterparts; DPPC-25°C < DPPC-50°C. Among the PEs, hydration increases with chain heterogeneity and degree of polyunsaturation; POPE < egg PEt < egg PE. Between SOPC and DOPC, SOPC with one unsaturated bond seems to hydrate less than DOPC which has two.

Other kinds of lipid mixtures. These show disproportionate degrees of hydration, not easy to correlate to polar group structure. Comparisons of the proportionate calculated values with observed values of V_{wo}/PE for the 1/1 mixtures of DGDG/POPE, DGDG/SOPC, and SOPC/POPE are shown in Table II.

Addition of non-polar lipids to bilayers. Cholesterol or diacylglycerol (DAG), which can be considered to act as lateral spacers between polar groups, cause large increases in water uptake per polar group mass. Thus, cholesterol added to DPPC at low levels, so that most of the hydrocarbon chains are still in the gel state, results in a large increase in hydration [43]. Addition to the extent of disordering the chains at room temperature gives hydration levels equal to that of the melted state. Equimolar levels of cholesterol [38] or 12 mol% DAG [42] added to egg PC results in hydration levels somewhat larger than pure egg PC. To pressures of 10^8 dyne/cm^2, McIntosh et al. [44] report little effect in pressure vs. separation for egg PCs to which cholesterol has been added up to 1:1 molar ratios. Given the lateral dilution of polar groups by cholesterol [45], this again shows increased hydration normalized per polar group.

TABLE II

1/1 mixtures of lipids V_{wo}/PE - proportionate/observed

POPE	SOPC	DGDG	
323	495/651	326/385	POPE
	667	497/467	SOPC
		328	DGDG

IV. Forces between lipid bilayers

Even to choose the mathematical form for describing pressure versus separation, one must be aware of at least four different kinds of interaction expected to occur between bilayers: the hydration force due to perturbations of water by the polar surface, van der Waals attraction that limits multilayer hydration, repulsion due to thermal undulations of the whole bilayer, and possibly steric interactions of polar groups whose conformations are confined by an approaching surface. In the sense that these all involve a positive or negative work to remove water between bilayers, they are all 'hydration forces' of some kind. The challenge is to estimate the relative contribution of each to the total energy. Each of these interactions will be considered in more detail below. The problem with any empirical description is to decide how to fit an experimental curve that can be fit with a minimum of parameters, with a set of postulated interactions that involve many more. Little can be learned using more than the minimum required parameters.

We emphasize here a minimum parameter description of the measured force curves. Plots of pressure as log P vs. separation d_w (Figs. 6–9) all suggest exponential decay of repulsive forces at high pressures, then a drop to a limiting separation, d_{wo}. A minimum description of the exponential part is given by

$$P_0 \exp(-d_w/\lambda)$$

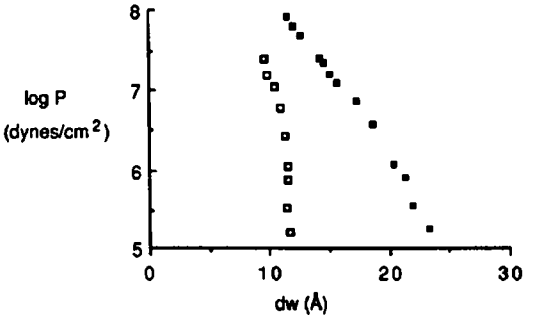

Fig. 6. Comparison of pressure vs. separation for POPE (open squares) and SOPC (solid squares) both at 30°C. Note the difference in range and slope (cf. Table I). Both lipids undergo phase transitions at pressures above those shown here.

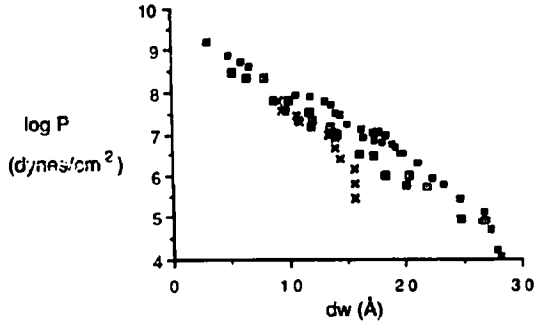

Fig. 7. Pressure vs. distance measured for egg PEt and its methylated derivatives. (×) egg PEt; (open square) singly (square with dot) doubly and (solid square) fully methylated. The greatest change is caused by the first methylation.

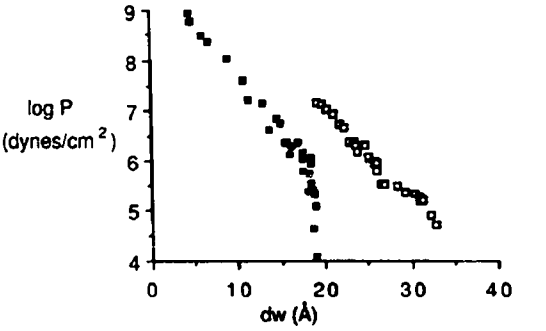

Fig. 8. Effect of chain melting on hydration repulsion. DPPC at 50 °C (open squares) and at 25 °C (solid squares). The 50 °C data are limited to log $P \leq 7$, since further dehydration causes acyl chain freezing.

Whether we fit to the full curve using this exponential plus an attractive van der Waals potential to enforce the 'hydration minimum' at d_{wo}, or we fit an exponential to the upper part alone, there is no qualitative effect on the extracted λ and P_0. These parameters do give, respectively, a good comparative measure of the range of the repulsive force as well as the strength it is expected to reach at a given separation. From these one can extrapolate the energy per unit area (or per molecule) that is encountered when two bilayers approach. What remains is to determine the contribution of each separate underlying force with an aim to understanding its physical origin [36].

Decay constants, λ, do correlate in a systematic way with polar group identity and state of the hydrocarbon chain. Again, using compressibility-adjusted estimates (Table I), statistical tests of the decay lengths [36] show that with a probability of > 98%, these decay lengths are in the sequence

POPE < egg PEt = egg PE < egg PEt-Me = egg PEt-Me_2 = egg PC = *SOPC*.

One sees that all the PEs (POPE, egg PE, egg PEt) have λ values of 0.8–1.3 ångströms, a range that includes decay rates for the two frozen-chain PCs (DPPC-25 °C and DSPC). Decay constants for the melted chain PCs, with the exception of egg PC/cholesterol 1:1, are 1.5–2.4 ångströms. λ for DGDG is somewhat closer to those for PCs.

As with total hydration V_{wo}, when compared within related lipid species, there is a striking effect of methylation on λ (Fig. 7, Table I). A single methylation changes the value from 1.1 ångströms for egg PEt to 1.8 ångströms for the monomethyl egg PEt-Me and the dimethyl egg PEt-Me_2 compared to 2.1 for the full methylated egg PC. And a 9:1 POPE/SOPC mixture shows a λ of 1.3 ångströms compared to 2.1 ångströms for a 2:1 mixture. Chain melting (Fig. 8) and increased chain heterogeneity (Fig. 9) increase bilayer hydration, seen in terms of force curves, just as they do in terms of maximum water absorption.

V. Hydration free energy

It is important to recognize that the dehydration measurements made under osmotic stress are in fact a direct measure of the free energy of the lipids as a function of the amount of water. Because lipid phase transitions usually involve significant changes in water content, these measured free energies can be a useful source of information in examining the phospholipid-water phase diagram and in testing various models of phase transitions. Guldbrand et al. [48] were the first to recognize this possibility in a model of the gel to liquid crystal transition. Leibler and Goldstein have recently developed an order parameter formalism to include hydration energies in this same transition [49]. Cevc and co-workers have performed practical and imaginative

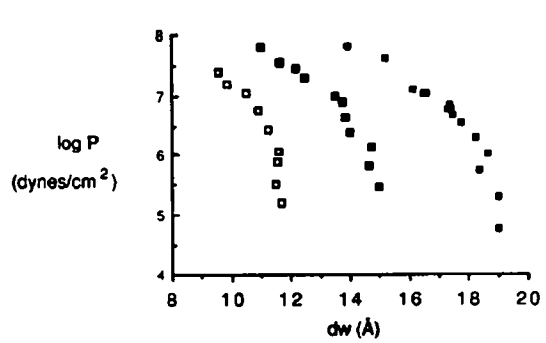

Fig. 9. Comparison of forces between bilayers with identical (PE) polar groups but different hydrocarbon chains. (open square) synthetic POPE, (solid square) natural egg PE, (square with dot) a derivative egg PEt made by transphosphatidylation of egg PC. Chain heterogeneity and degree of polyunsaturation increase the tendency of PE hydration [36].

measurements of the temperature and entropy of this same transition as a function of water content [50,51]. Since we believe that this kind of analysis is just the beginning of many possible uses of dehydration/phase transition data, we have codified the data on bilayer dehydration in terms of osmotic stress vs. water volume parameters [36]. The enormous energies of bilayer dehydration may be appreciated by examining one case, e.g. egg PC, where forces have been measured virtually to zero water. Taking λP_0 as a measure of the integrated work, one sees (Table I) that at a pressure of 10^9 dyne/cm^2, for example, dehydration has involved a work of some 20 erg/cm^2, and that for bilayers approaching zero-water contact this energy can grow to the order of 100 erg/cm^2. Translated into chemical units, this amounts to 2–10 kcal/mol (8.4–42 kJ/mol). These energies are of the magnitude known for oil-water of vapor/liquid contact.

VI. Measured bilayer adhesion energies

Phospholipid hydration, preventing anhydrous contact, is an important factor affecting the strength of adhesion between electrically neutral bilayers. For this reason, the measured strength of adhesion between bilayers can be a useful inverse indicator of the strength of bilayer hydration. The pipette aspiration method provides the most direct measure of the energy (negative) per unit area, G_{min}, of spontaneous interaction between bilayers. The measured contact angle, θ, and applied bilayer tension $\bar{T}$ in the bilayer give, by Young's equation [76],

$$G_{min} = 2\bar{T}(\cos\theta - 1)$$

One can combine this G_{min} with an estimate of average bilayer separation d_{wo} measured by X-ray diffraction. This combination allows one to test various models for bilayer attraction forces and to correlate strength of adhesion with hydration force measurements [18,37].

The osmotic stress measurement alone allows a second estimate of contact energy, but it relies on an extrapolation of the exponential repulsive force

$$P_0 \exp(-d_w/\lambda)$$

to the position, d_{wo}, where this force is equal and opposite to a longer range attractive force. For example, if one assumes the distance dependence of van der Waals attraction in its simplest form, one has [10]

$$F_{vdw} = A_h/(6\pi d_w^3)$$

TABLE III

Bilayer-bilayer adhesion energies derived by three methods.

Osmotic stress (OS) extrapolations assume a simple $1/d^3$ van der Waals attraction. Agreement of all three methods is excellent for digalactosyldiacylglycerol but not for PEs or PCs. Osmotic stress (OS) and pipette aspiration (PA) measurements are on unsupported films. Undulations of these films might explain some of the difference from surface force apparatus (SFA) measurements for the PCs and PEs, but most of these differences are not understood. (Source references are in square brackets. OS values are from Table I.) Temperature is taken to be at 25°C unless stated otherwise. G_{min} tabulated are absolute values of negative quantities (erg/cm^2).

Lipid	SFA	PA	OS
eggPC			0.01
DLPC	0.1 (22°C) (52)	0.01–0.015 [17]	0.01 (25°C)
SOPC		0.012 [a] [18]	0.02 (25°C)
DMPC			0.02 (27°C)
DPPC	0.15 (21°C) (53)		0.03 (25°C)
DPPE	0.80 (Lβ) (53)		
POPE		0.12–0.15 (Lα) [18]	0.14
DGDG	0.29 (53)	0.25 [37]	0.24
MGDG	0.48 (29)		

[a] When accounting for undulation forces present in the OS and possibly in the PA and absent in the SFA bilayers, 0.012 erg/cm^2 becomes 0.0165 erg/cm^2 (E. Evans, personal communication).

as indicated from SFA measurements [29,52,53]. Then, integrating these two forces from infinity, one infers

$$G_{min}(d_{wo}) = F_{vdw}(d_{wo}) \cdot ((d_{wo}/2) - \lambda)$$

At d_{wo},

$$F_{vdw}(d_{wo}) = P_0 \exp(-d_{wo}/\lambda)$$

so that

$$G_{min}(d_{wo}) = ((d_{wo}/2) - \lambda) \cdot P_0 \exp(-d_{wo}/\lambda)$$

which can be evaluated from measured P_0, d_{wo} and λ.

As long as the attractive force is of much longer range than the repulsive one, the order of magnitude of G_{min} extracted by this procedure is not very sensitive to the form of attraction. For example, if one includes the finite bilayer thickness or even subdivides the bilayer into regions of different polarizability [10], estimates of G_{min} will not be qualitatively affected.

The force F_0 at the position of maximum attraction where two phospholipid-coated mica surfaces jump together in the SFA gives yet a third way to measure G_{min} [52,53]. By the Derjaguin approximation (see Fig. 4 and related text),

$$G_{min} = F_0/2\pi R$$

In Table III we have compared estimates from these three methods. What is puzzling is the much greater estimate of G_{min} from the coated mica surface measure-

ments compared to those between unsupported bilayers. In any case, all these minima are $\lesssim 1$ erg/cm^2, relatively weak on the scale of oil/water or vapor/liquid interfacial energies.

VII. Hydration of charged phospholipid bilayers

Because of the high pressures produced by combined hydration and electrostatic double layer forces, hydration interactions between charged phospholipids are not always easy to see. With the OS method, it is necessary to apply high stress and go to small spacings, especially in solutions of low salt concentration, in order to observe deviation from pure electrostatic repulsion. Often such pressures cannot be attained with the SFA before there is bending of the supporting mica surfaces. For example, measurements of forces between distearoylphosphatidylglycerol (DSPG) in NaCl solutions, using the surface force apparatus, were limited to separations greater than 20 ångströms, a separation too large and at pressures too low to observe hydration repulsion [31].

It is worth considering where one should see a transition from electrostatic double-layer-dominated repulsion to a regime of hydration force dominance (Fig. 10).

Consider, for simplicity, an electrostatic repulsion between parallel surfaces, separated by a distance d, of the form

$$P_{es}(d) = P_{es}\exp(-d/\lambda_e)$$

where P_{es} depends on surface charge and the decay

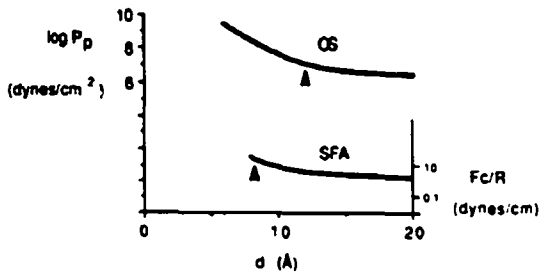

Fig. 10. Difficulty of detecting hydration forces between charged bilayers. The sum of the electrostatic and hydration repulsion is plotted as a pressure, P_p, between parallel surfaces, or its integrated equivalent, F_c/R between crossed cylinders of radius R; $F_c/R = 2\pi E_{pp}$ where E_{pp} is the energy between parallel surfaces. Parameters used are, for hydration repulsion similar to that between PEs, $\lambda = 1$ Å, $P_0 = 10^{12}$ dyne/cm^2; and for the electrostatic double layer, made so that $P_{es} = P_{hyd}$ at 12 Å with Debye length of 10 Å. Lines are drawn over regions accessible to osmotic stress, P_p, and to the surface force apparatus, F_c/R, without deformation. Note the shift in the position of switchover from electrostatic double layer to hydration force (arrows). Theoretical curves omit contribution of undulatory fluctuations.

distance λ_e is the Debye-Huckel decay length. Add to this a hydration repulsion of the form

$$P_{hyd}(d) = P_0\exp(-d/\lambda)$$

Between *parallel* surfaces, then there will be a transition from electrostatic to hydration forms around a position d_p where these two quantities are of comparable magnitude,

$$P_{es}\exp(-d_p/\lambda_e) = P_0\exp(-d_p/\lambda)$$

or

$$d_p = ((\lambda\cdot\lambda_e)/(\lambda_e-\lambda))\cdot\ln(P_0/P_{es})$$

This separation d_p will typically be less than the maximum distance assumed by neutral bilayers of comparable hydration tendency.

Between oppositely curved surfaces, such as the crossed mica cylinders, this transition will occur at a separation d_c where the integrated *energies*, $\lambda_e P_{es}(d)$ and $\lambda P_{hyd}(d)$ are comparable. That is

$$\lambda_e P_{es}\exp(-d_c/\lambda_e) = \lambda P_0\exp(-d_c/\lambda)$$

so that

$$d_c = ((\lambda\cdot\lambda_e)/(\lambda_e-\lambda))\cdot\ln((\lambda P_0)/(\lambda_e P_{es}))$$

$$= d_p - ((\lambda\cdot\lambda_e)/(\lambda_e-\lambda))\cdot\ln(\lambda_e/\lambda)$$

The effect of opposite curvatures is to shift in toward contact the place where hydration forces 'take off'. Except for solutions of very high (i.e., molar) salt concentrations, $\lambda_e \gg \lambda$, and this shift is approx.

$$d_c - d_p = \lambda\cdot\ln(\lambda_e/\lambda)$$

This is some 3 to 8 hydration decay lengths in solutions of 100 to 1 mM ionic strength, respectively. This represents a non-trivial difference in the stress required to observe hydration forces between oppositely curved surfaces, as illustrated in Fig. 10.

Although hydration repulsion between charged bilayers has not been as thoroughly examined as that between neutral bilayers, there is clear evidence of an extra non-electrostatic repulsion. Early measurements of egg PG/egg PC and erythrocyte PI/egg PC mixtures under osmotic stress in zero-salt solutions showed an extra repulsion at small separations that were taken to indicate hydration repulsion [54]. The deviations from electrostatic repulsion at 5 and 10 mol% PG or PI almost exactly followed the curve for pure egg PC at the same separations. The very high forces encountered with pure PG at close separation are similar to those seen with egg PC hydration, but a purely electrostatic explanation cannot be ruled out (J.N. Israelachvili, personal communication).

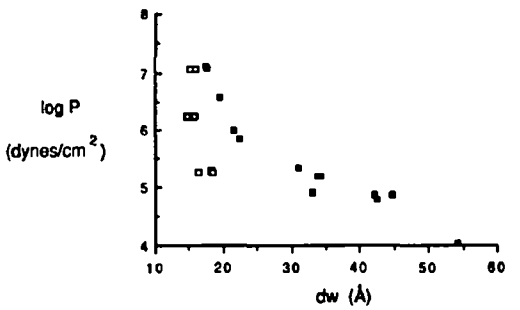

Fig. 11. Interbilayer pressure between PS bilayers as it varies with separation in (□) 1.0 M NaCl, (■) 0.4 M NaCl. For 0.4 M NaCl, the sudden onset of a repulsion at about 20 Å gives a much steeper slope than expected from electrostatic decay.

Evidence of an extra, non-electrostatic force is much less ambiguous in measurements on pure egg PG and egg phosphatidylserine (egg PS), in 0.01 to 1.0 M univalent salt solutions [55]. Both materials showed the sudden onset of a repulsion at some 20 Ångströms separation, of a much steeper slope than expected from electrostatic decay, and apparently unscreened even by high salt concentrations (Fig. 11).

In retrospect, these data suggest a non-electrostatic double layer repulsion more like that between egg PE bilayers than between egg PC bilayers. In fact, we have recently found that DOPS in 0.8 M NaCl swells like egg PE, a repulsion that becomes important at an about 14 ångström separation and varies with the approx. 1–2 ångström decay rate of egg PE. The opportunity exists for further measurement in these and related systems.

We have recently measured forces between bilayers of the non-phospholipid, dihexadecyldimethylamine acetate (DHDAA) in 5–500 mM acetate solutions. In 5 mM acetate solutions, for example, there is a clear break away from electrostatic double layer repulsion at an 11 ångström separation and at a pressure of $6 \cdot 10^6$ dyn/cm^2. Below this separation there appears to be an exponential repulsion much like that of POPE. The integral of this force curve corresponds nicely with what one sees with the SFA [56] where, between curved surfaces, there is primarily electrostatic interaction with no break down to a separation of 5 ångströms. This comparison illustrates well the implications of the shift inward of the hydration take-off point for oppositely curved surfaces relative to parallel surfaces.

Qualitatively, different kinds of interaction occur between acidic phospholipid bilayers exposed to divalent cation solutions. The many studies of such systems show that the interactions are strong enough to break through the hydration barrier and allow very close contact. Much use has been made of this in attempts to model membrane fusion. An example of such a remarkable change occurs in PS bilayers exposed to Ca^{2+} ions. Even at micromolar Ca^{2+} concentrations, these bilayers precipitate to virtually anhydrous contact often with crystallization of hydrocarbon chains [57–59]. By comparing the binding constant of Ca^{2+} to the outer surface of multilayers [60] with the strength of binding between bilayers [58], we estimate an energy of contact on the order of 100 erg/cm^2 in these Ca^{2+}-collapsed PS multilayers, quite enough to completely overcome hydration repulsion. (Method of Parsegian and Rand [61] updated with the binding constants of Feigenson [58].) The fact that this precipitate contains no detectable water argues against an attractive force based on ionic fluctuations [62,63] and suggests, rather, the kind of dehydration characteristic of insoluble ionic crystals.

VII. Amplification of bilayer repulsion by undulatory fluctuations

For some time, since the pioneering work of Helfrich [64] on steric repulsion between lipids, there has been the sense of a dilemma in deciding whether lipid bilayers repelled because of actual forces between them or because of collisions that occurred when they experienced normal thermal undulations. It appears now [65,66] that there is no dilemma. Bilayers do undulate. These undulations are suppressed by long-range interactions rather than the hard collisions originally imagined. And the loss of undulatory entropy, suppressed by membrane repulsion, is an important part of bilayer packing energy.

There appear to be two limiting regimes: one where bilayers are so close that undulations are effectively suppressed and bilayers interact only through the underlying or direct interbilayer repulsive force; another where bilayers are sufficiently far apart that forces between them are weak enough and of relatively short enough range for them to repel as predicted by the original Helfrich model [67]. In between, there is a coupling of steric undulatory and underlying or bare interactions that results in behavior different from either taken alone.

To clarify the relative strength of bending undulatory and direct interaction forces, it is worth examining the form of the undulatory fluctuation force, P_n, in a regime where the underlying interaction is dominated by a single exponentially decaying force

$$P_0 \exp(-d_w/\lambda)$$

In that case

$$P_n = (\pi kT/32\lambda)\sqrt{((P_0/B\lambda)}\exp(-d_w/2\lambda))$$

(To derive this result, see Ref. 66. Introduce Eqn. 18 or 19 into Eqn. 16 or into the derivative of Eqn. 14 of that paper.) Here, B is the bilayer bending modulus (usually about 25 kT) and λ and P_0 are the decay rate and coefficient of the underlying repulsion. For dis-

tances, d_w, much bigger than λ, this fluctuation component will dominate to give a force that decays half as fast as the underlying force. It is possible at these larger distances to infer the actual bilayer–bilayer interaction only through a theoretical construct that takes the undulatory force into account.

It is instructive to compute the point of crossover between the dominance of a direct exponential force

$$P_o \exp(-d_w/\lambda)$$

and the undulatory fluctuation force. Set

$$P_0 \exp(-d_w/\lambda) = (\pi kT/32\lambda)\sqrt{((P_0/B\lambda)}\exp(-d_w/2\lambda))$$

For $\lambda = 2$ ångströms, $P_0 = 10^{10}$ dyne/cm^2, $B = 25\ kT = 10^{-12}$ erg, equality is satisfied for $d_w \approx 17$ ångströms. Below this distance, one would not expect appreciable contributions from fluctuations. At greater distances, one may see expanded exponential decay due to fluctuations.

Indeed, recent measurements of forces between parallel DNA double-helical linear polyelectrolytes [68] show precisely this halving of the decay rate. In salt solutions of low concentration, but at separations much greater than the Debye length, forces vary with half the classical Debye decay rate. In very high salt concentrations, where charge interactions are screened, there is an exponentially varying hydration force at separations less than 10 ångströms and an extended region of half the decay rate at greater separations. Simultaneous measurement of molecular motion indicated by progressive broadening of the X-ray reflections, confirms that the region of extended decay corresponds to a regime of steadily increasing molecular motion.

In general, the interplay of direct forces and undulatory fluctuation forces will not always result in cleanly visible behavior of one or the other type. Between phospholipid bilayers which enjoy undulatory freedom near the position of force balance between van der Waals attraction and hydration repulsion, the action of fluctuations seems to be to amplify hydration repulsion near the limit of swelling. Fluctuations shift the force balance outward [66].

Fortunately, it is possible to compare experimentally measured forces between bilayers undulating within a multilayer array with those between bilayers immobilized onto rigid mica cylinders, where undulations are presumably impossible. Fig. 12 shows the force vs. distance between bilayers on crossed mica cylinders, differentiated to give the equivalent force per molecule F_R (shaded band), together with measurements of repulsion between bilayers in a multilayer array, also as a force per molecule (points). Both data sets are for PCs with melted hydrocarbon chains. It is clear that in a region of strong repulsion the two show similar forces

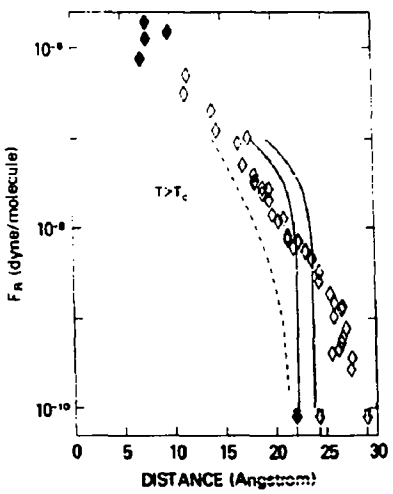

Fig. 12. Comparison of forces measured between bilayers in a multilayer (◇) using osmotic stress and between bilayers immobilized onto the crossed mica cylinders of the surface force apparatus (shaded band). The data points are for DLPC at 25°C where hydrocarbon chains are melted except at high pressure (◆). Data from Ref. 38. The SFA curves are for a set of melted chain PCs [32,52]. The dashed line is the underlying interbilayer force after subtraction of undulatory fluctuation forces in the multilayer system [66]. Arrows indicate limiting spacing at zero force. This plot shows (a) the expansive power of undulatory steric fluctuations in the regime of small pressures (lower third of figure), (b) the suppression of these fluctuations at higher pressures, (c) the remarkable agreement SFA and OS measurements once one takes account of the difference in apparent zero of separation. (F_R is force per molecule. For details see Ref. 32.)

with only a small horizontal shift due probably to differences in the defined 'zero' of separation. But at low pressures there is a distinct divergence between the two data sets; the limiting spacing of the multilayers is considerably greater than that between adsorbed bilayers. If, though, one subtracts undulatory entropic contributions from these data using the theory of Evans and Parsegian [66], one obtains the dashed line that is remarkably parallel to the fixed-bilayer shaded band of the SFA measurements [32].

This comparison actually teaches us at least two things. First, undulations act to enhance the hydration force giving it a greater apparent range. Second, at higher pressures undulations are effectively suppressed, suggesting that one can use measurements in this range to estimate the underlying hydration force.

There are cases where fluctuations probably always dominate the repulsion of weakly hydrating bilayers such as the case of the non-ionic alkylpoly(oxyethylene) (PEO) surfactants. Tiddy and coworkers have used controlled vapor pressure to measure forces between bilayers of compounds of various hydrocarbon and ethyleneoxide lengths. Tiddy et al. [69,70] argue that the polyethylene oxide chain polar groups are extended and probably hydrate with only one layer of water, and

within their residence space form a PEO/water mush. Melted bilayers separate to greater extents than when they are frozen. Melted bilayers of the shorter chain compounds swell appreciably more than the longer chain species, which are presumably less flexible, and achieve separations greater than the maximum length of the fully extended amphiphile molecule. There is good reason then to think that these long spacings occur from undulatory fluctations confined by collision between the hydrated polar regions of facing bilayers [69,70].

IX. The vapor pressure paradox

Widely recognized among phospholipid physical chemists, and even more widely ignored among those who prepare lipids for laboratory study, is the fact that lipids exposed to a water vapor of 100% humidity will not take up as much water as will the same sample put into contact with liquid water (Refs. 41, 71, 72, compare to Table I). Typically, for example, a phosphatidylcholine multilayer will imbibe some 45–55% (w/w) water from the pure liquid but only some 30% from a water-'saturated' vapor [52,72]. What is more, a sample equilibrated against liquid will actually give up water to a 100% r.h. vapor and then reversibly regain water from a liquid when given an opportunity to do so. (Rand, R.P., unpublished results; Gruner, S. and Templar, R., personal communication).

Worse, a charged phospholipid, e.g., phosphatidylserine [71] that will swell indefinitely to isolated bilayers in liquid water [55] will actually stop swelling in vapor at a water content far less than that taken up by phosphatidylcholine under similar conditions [71]. The limit of swelling of multilayers on solid substrates (Ref. 73 and Gruner, S. and Templar, R., unpublished results) seems to resemble that of lipids in vapors.

What is going on? Isn't the activity of a 100% r.h. vapor the same as that of the liquid water with which it is supposed to be in equilibrium? One's first thought is that perhaps, because of slight thermal gradients, the vapor activity is somewhat less than that of its mother liquid. Consider the osmotic stress Π equivalent of a vapor of relative humidity p/p_0.

$$\Pi = -(kT/v)\ln(p/p_0).$$

where v is the 30 Å^3 volume of a water molecule and $(kT/v = 1.4 \cdot 10^9$ dyne/cm^2. For p near p_0, we may write $p/p_0 = 1 - \Delta$ and

$$\Pi = (kT/v)\Delta = (1.4 \cdot 10^9)\Delta.$$

An osmotic pressure of 10^6 dynes/cm^2, enough to remove 1/3 to 1/2 the water from a multilayer, is given when $\Delta = 0.00075$, or the relative humidity is more than 99.9%, which could come from a 0.01°C dip in the temperature! See Fig. 13 for the great effects that small changes in relative humidity, resulting from tiny temperature fluctuations, can have.

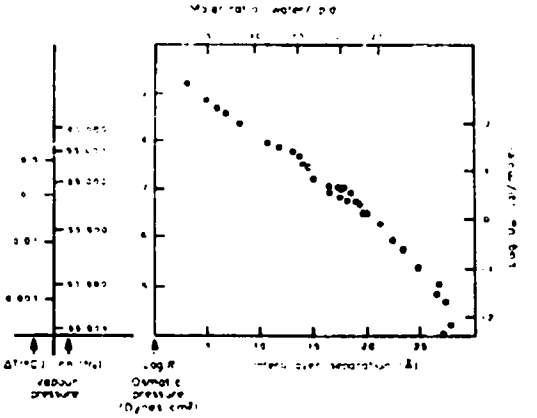

Fig. 13. Molar ratio (water/lipid) and bilayer separation for eggPC bilayers plotted as function of pressure expressed four different ways: (i) osmotic stress dyne/cm^2; (ii) chemical potential, μ_w, relative to bulk water; (iii) equivalent relative humidity; (iv) temperature increase that would correspond to the same changes in equivalent relative humidity and osmotic stress.

Temperature fluctuations will explain the escape of water from bilayers in liquid to vapor. But thermal fluctuations do not explain the observation that water is lost to a vapor maintained at 110% relative humidity. In that experiment water-saturated air was cooled before being blown at a hydrated sample (Gruner, S., personal communication).

A second possibility therefore is that the action of a vapor/multilayer or solid/multilayer interface is to suppress the bilayer undulations that enhance hydration or electrostatic repulsions. Quantitative comparison of water loss in vapor with the predicted shift in equilibrium spacing using the model of Evans and Parsegian [66] suggests that, considering present theories, one can account for about one half of the observed effect via this explanation.

Other possible explanations might recognize the restraining effects of high surface tensions. The results of Safinya et al. [74] on planar lipid films stretched over a hole and exposed to vapor show that the geometry of the overall multilayer is not critical.

The inability of charged lipids to swell in vapor suggests to us that the phenomenon is at the very least a practical problem. One knows that charged lipids must repel. If this swelling is unwittingly prevented, a handling problem is certainly evident. On preparing samples in vapor, one should be suitably aware that, under these conditions, lipids will not go to full hydration.

X. Interaction between oppositely curved bilayer surfaces: vesicle interaction and deformation

Very often one must know the interaction between bilayers that are in the form of vesicles or curved surfaces. We emphasize here that the form of interaction will depend on whether the curved surfaces are parallel to each other or whether they curve away from each other (have the opposite curvature) as they necessarily do in vesicle–vesicle and vesicle–plane interactions. It is also clear that the forces encountered are strong enough to deform interacting bilayers, to restrain thermal undulation, or to flatten neighboring vesicles. It is instructive to see how hydration repulsion and the adhesion energy, G_{min}, between parallel surfaces at a position of force balance, show up in the interaction between curved surfaces. These phenomena have been examined rigorously by E. Evans and co-workers [16–18,20–22,24].

As described above, a convenient approximation due to Derjaguin [30] allows one to transform forces measured between parallel planar layers (pp) to interactions expected between spherical vesicles (ss) or spherical vesicles and flat layers (sp). Between crossed cylinders of radius R or between a sphere of radius R and a plane, the force F_{sp} is related to the energy E_{pp} by

$$F_{sp}/R \approx 2\pi E_{pp}$$

Between two spheres, the transform is

$$F_{ss}/R \approx \pi E_{pp}$$

It is remarkable that the point d_0 of zero net force or minimum energy is the same between two spheres, between a sphere and a flat layer, or between two crossed cylinders, and is quite independent of radius R. Further, this d_0 between oppositely curved surfaces will always be expected to occur at a smaller separation than between parallel surfaces. (cf. Fig. 4, $E_{pp} = 0$ at a smaller separation than where $F_{pp} = 0$.) The interaction between surfaces which curve away from each other is a sum of individual interactions at different separations. In the Derjaguin approximation some parts of the surface may feel net attraction, some repulsion. The longer range force will be felt over a greater area of the surface than the repulsive. It will have a proportionally large 'say' in determining the final position of force balance. (For an illustration of the result of mixed attractive and repulsive electrostatic double layer forces between spheres, and a rigorous examination of the accuracy of the Derjaguin approximation for such interactions, see Ref. 75.) But this same combination of attraction and repulsion will create a torque to deform a curved surface. One must therefore recognize surface deformability in any problem involving curved surfaces.

What can one say at the level of vesicles of 200 ångström radius? First, between rigid spheres compared to parallel layers, there will be an inward shift in the position of force balance between long-range attraction and short-range repulsion. Second, since vesicles are in fact not rigid, they will flatten to create regions of planar adhesion having the energy, G_{min}, per unit area described above.

Rigid spheres

For simplicity, consider a repulsive force of the form $P = P_0 \exp(-d/\lambda)$ and attraction of the van der Waals form $F_{vdw} = -(A_h/6\pi d^3)$. (Here we use d as the distance between the surfaces. By virtue of the assumption of rigidity, one ignores any action of undulatory repulsion.) The corresponding energy between two planar surfaces experiencing these forces is

$$E_{pp} = \lambda P_0 \exp(-d/\lambda) - A_h/(12\pi d^2)$$

$$= (\lambda \cdot P) - (d/2) \cdot F_{vdw}$$

Sketches of force and energy per unit area for typical parameters (Fig. 14) show the inward shift in zero-force position for spheres or cylinders from that for parallel planes.

Since the force between spheres goes as the radius R, the depth of the energy minimum for interacting spheres is proportional to sphere radius. By $F_{ss} = \pi R\, E_{pp}$, the energy of interaction between two spheres is represented as

$$E_{ss} = (\lambda^2 P_0 \exp(-d/\lambda) - A_h/(12\pi d))\pi R$$

$$= ((\lambda^2 \cdot P) - (d^2/2) \cdot F_{vdw})\pi R$$

The fact that the minimum energy position of two spheres is at a separation less than that of two parallel planes means that the closest parts of the spheres are actually being pushed to a separation where they repel (Fig. 14). The simultaneous attraction and repulsion on different parts of a vesicle create a torque that can be relaxed by vesicle deformation.

Deformable vesicles

The stress of hydration repulsion and even weak van der Waals attraction is such that virtually any curved bilayer surfaces must deform to some extent when in adhesive contact [76]. Lateral tension $\bar{T}$ within the bilayer surface develops against the drive to create a flattened area of contact of adhesive energy, G_{min}, in such a way as to satisfy Young's Eqn. and to make a contact angle θ (Fig. 15).

$$\cos\theta = 1 + (G_{min}(-)/2\bar{T})$$

For small contact angles $\cos\theta = 1 - \theta^2/2$ and

$$\theta^2 = -G_{min}(-)/\bar{T}$$

The area of flattening $\pi R^2\theta^2 = \pi R^2 G_{min}(-)/\bar{T}$, the fractional area of flattening is

$$\pi R^2 G_{min}(-)/(\bar{T}4\pi R^2) = G_{min}(-)/4\bar{T}$$

and the energy of interaction over this flattened area is

$$\pi R^2 G_{min}(-)^2/\bar{T}.$$

The factor of 10 difference in G_{min} between PE and PC leads to a factor of 100 difference in the contact energy between deformable vesicles. For example, consider an $R = 200$ Å vesicle under tension $\bar{T} = 1$

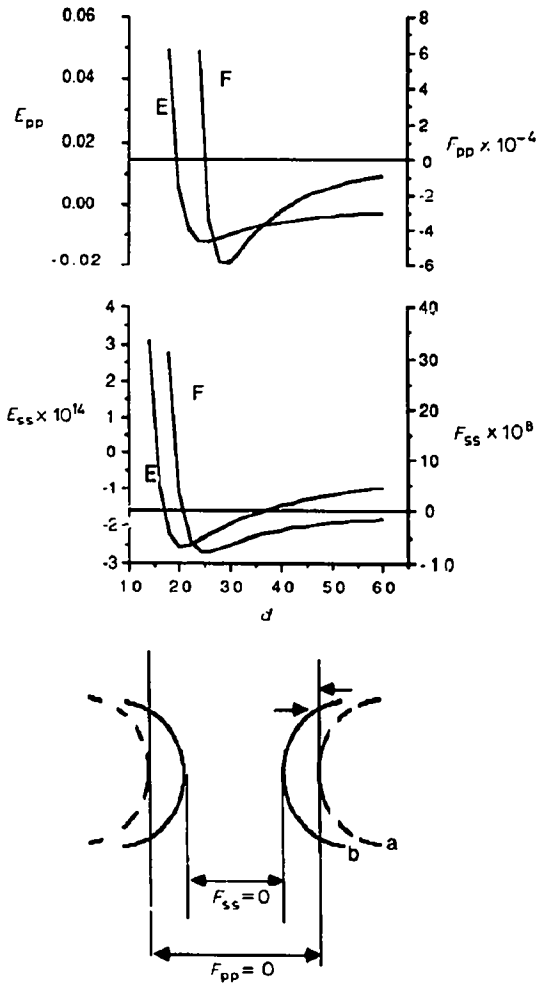

Fig. 14. Simultaneous attraction and repulsion between rigid spheres occurs at a minimum energy position which is less than that of force balance $F_{pp} = 0$ between parallel planes of the same material. (a) Spheres at separation corresponding to maximum attraction; (b) spheres at their minimum energy separation (where $E_{pp} = 0$). Small arrows show conflicting repulsive and attractive pressures creating a torque on curved surfaces.

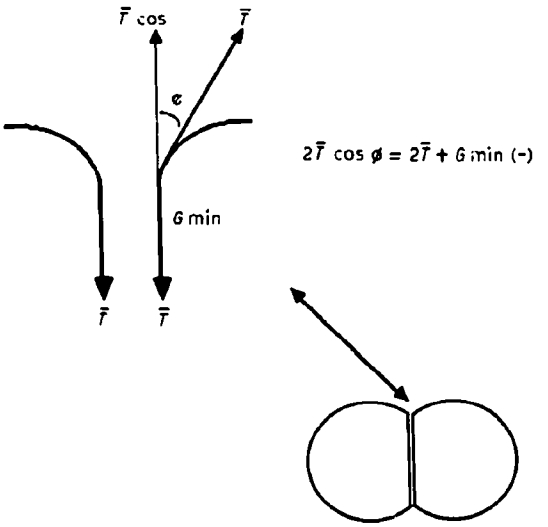

Fig. 15. The balance of line tension $\bar{T}$ and attractive energy $G_{min}(-)$ to create a deformed region of phospholipid vesicle interaction. $G_{min}(-)$ between neutral phospholipids is usually pictured as a balance between van der Waals attraction and hydration repulsion. Despite the tension developed, there may be some repulsion also from undulatory fluctuations. Between some phospholipids there may also be hydration attraction or H-bonding across a water layer due to complementary surface polar groups.

dyne/cm. The adhesive interaction for $G_{min} \approx -0.01$ erg/cm^2 will be only 1/5 of the thermal energy $kT = 4.2 \cdot 10^{-14}$ erg.

But for $G_{min} \approx -0.1$ the interaction energy will be some 20 kT.

Depending on tension, the contact energy will often be dominated by G_{min} · area of contact.

Other contributions, such as the residual attraction between non-flattened areas and the work of deformation will very often be small by comparison. When vesicles are deformable, as is usually the case with phospholipids, their interaction is more characteristic of forces between parallel planes than between curved surfaces. It is puzzling to us why most models of vesicular aggregation neglect this important feature of interaction.

XI. Hydration in other systems

It was our purpose in this review to collect information strictly on phospholipid bilayer hydration, information that has become available from different experimental methods. It would be wrong, though, not to mention for reference what is being learned in other systems.

All modern studies of solvation and hydration follow the major achievements of Derjaguin and his school. It was these people who built and designed the first suc-

cessful surface force apparatus, developed much of the physical theory of long-range forces, and recognized the importance of the 'structural component of the disjoining force' (for which read 'solvation' or 'hydration' repulsion). This work is the subject of a book and several recent reviews [2–5].

The swelling of clays, by the action of both electrostatic and hydration forces has been recognized for several decades. Early work examining layer spacings as a function of vapor pressure [77] showed multiple spacings that gave a first indication of discrete layering of water on hard smooth surfaces. Studies during the past two decades, particularly those of Low and collaborators (e.g., Ref. 78 from which references to the very large amount of earlier literature may be traced) have shown exponentially varying forces measured by osmotic stress. Closely related to these are the now extensive studies between mica surfaces using the surface force apparatus and reviewed recently by Israelachvili who is the principal designer of the present form of the apparatus [79]. In particular, measurements by Pashley, Israelachvili and coworkers have found that mica–mica interactions are often oscillatory with an oscillation period corresponding to the dimensions of intervening solvent. We take it to be significant that oscillatory forces have not been seen between bilayers or between macromolecules in solution; the smoothness and hardness of the mica or clay surface probably creates a different perturbation of solvent than is effected by the relatively flexible groups that make up most lipids and large molecules. Pashley has also found many instances of 3–10 ångström exponential decay which is interpreted as due to 'secondary' hydration of ions adsorbed to the mica surface [80,81]. Correlation with the clay swelling measurements is good, once account is taken of differences in definition of the 'zero' contact distance.

We have already mentioned the osmotic stress measurements of forces between DNA molecules [68,82]; one should mention as well similar force determinations on polysaccharides [83]. We note again the work on oxyethylene surfactants that seem to be dominated by undulatory repulsions between hydrated bilayers [69,70] and our recent measurements with charged dihexadecyldimethylamine acetates that show strong exponentially growing forces at less than 11 ångströms separation much as some synthetic phosphatidylethanolamines. The surface hydration of such bilayers has been well recognized by Ninham and Evans and collaborators for the many ways in which it influences lipid polymorphism [84,85].

We have written elsewhere of the relevance of hydration repulsion to bilayer fusion processes [86,87]. Forces measured between natural nerve myelin strongly resemble those seen between phospholipids although the cell surface is likely to be a far more complicated structure [88]. We will forego the temptation here to list the many biological phenomena that may relate to the hydration properties of molecular and membrane surfaces.

There have been several reports of a long-range 'hydrophobic' attraction detected in the SFA between mica surfaces coated with monolayers whose hydrocarbon chains face out onto the water region (e.g., Refs. 89 and 90 and references therein). This force has been detected to some 900 ångströms separation and shows exponential decay rates up to 160 ångströms [90]. Recent observations and arguments suggest the improbability of a solvent-mediated force of this range [90].

XII. Theoretical questions

Much effort has been spent to develop a satisfactory theory of hydration. In lipid systems, difficulties are compounded by the several phenomena affecting surface hydration. Bilayer undulation, lateral compressibility and deformation, polar group packing and rearrangement, all no doubt contribute to the wide range of force decay rates and works of dehydration that emerge in the comparisons presented here and debated in the current literature.

Why 'hydration' at all? Essentially because of the work encountered in bringing together neutral bilayers in distilled water or low salt buffers. Added salt seems to make relatively little difference except at molar concentrations [91]. Charged bilayers do interact in ways that suggest salt-screened electrostatic double layers, but only at distances greater than where strong forces are encountered between neutral bilayers. At shorter distances ($\approx$ 20 ångströms) charged bilayer repulsion usually resembles that between neutral phospholipid bilayers [55].

So, at the root level, a 'hydration' or 'dehydration' force implies a work of removal of water from between membrane or molecular surfaces. One could include in that work any steric forces of polar groups or of entire undulating bilayers, specific arrangements of polar groups that enable attraction as well as repulsion, and actual adsorption of water to the membrane polar groups. It is not clear when any of these factors stands out so clearly as to be distinctly identified. What is clear, though, is that it has not been possible to rationalize measured forces with any theory that neglects the structure of the intervening solvent.

For simplicity we still favor the approach originally proposed by Marcelja and coworkers [92]. A polar surface will perturb aqueous solvent just next to it; and the propagation of this perturbation by solvent–solvent interactions mediates a force that extends, with a solvent-characteristic length, over many solvent layers. The strength of interaction was seen as a function of the perturbing strength of the surface, while its exponential decay was a characteristic of the intervening solvent. The original formulation spoke in terms of an order

parameter of undetermined type. Gruen and Marcelja [93,94] emphasized the importance of water polarization, while later studies by Kjellander and Marcelja [95] examined the possibility of H-bond rearrangement within the water solvent or of the coordination of water molecules. The formulation of Ruckenstein and Schiby [96] emphasized the importance of surface polarization and water dipole interactions.

Cevc and coworkers [97,98] have argued for recognition of a hydration potential, a measure of the polarizing or hydrating power of polar groups, rather than a fixed value for the operative order parameter at the hydrating surface. This idea of a potential has been developed into an effective surface polarity, a function of polar group ionization, methylation or other surface parameters, that is responsible for reorganizing boundary water [99,100]. It has been possible to create a self-consistent model allowing a near-quantitative explanation of a large body of data on phase transitions [101,50]. Much of this material has been reviewed recently in some detail [99]. Simon and McIntosh [102] have argued recently that the surface potential, measured across phospholipid monolayers in presumed equilibrium with free multilayers, is the organizing potential that would fit into the Cevc et al. formalism. Since dipole potentials can be inferred from bilayer transport measurements, it seems worthwhile investigating this claim by direct comparison.

Kornyshev et al. [103] use a continuum dielectric formalism with a non-local response to rationalize the decay of hydration forces. In recent work, they have succeeded in coupling solvent correlation length with the lattice constant of interacting surfaces. The result is a net decay length that can be different for different surfaces interacting across the same solvent material [104]. Quite recently, Attard and Batchelor [105] have proposed a model that recognizes the progressive entropy loss (or enthalpy gain) of the surface-perturbed water H-bond network. Decay lengths reflect surface boundary conditions as well as solvent lattice lengths to allow some variation in decay rate. This approach emphasizes the non-electrostatic nature of the solvent parameter that mediates hydration forces.

Indeed, the continuous 1–3 ångström range of measured decay rates for forces between phospholipid bilayers suggests that a single-decay picture is either inadequate or results from being combined with other forces. Forces decaying exponentially with approx. 3 ångström decay constants have been seen much more consistently between linear polyelectrolytes [82]. Perhaps in these systems they can be more fruitfully analyzed theoretically.

Computer simulations of H-bonding water near polar surfaces [95] do not show the kind of extended decay of perturbation expected from the original Marcelja formalism or presumably from later H-bond models. But this may be due simply to the fact that these simulations are accurate to some 0.5 kcal/mol of solvent (e.g., Ref. 106) while the perturbations of water that seem to be important are as small as approx. 1 cal/mol (Fig. 13). Indeed, the essence of these forces, and the reason they were not expected from probes of water itself, is that they come from virtually indetectable perturbations of solvent summed over large numbers of water molecules. One can obtain some idea of the difficulty of modelling hydration forces by looking at the force distance curve in chemical rather than physical units. The right hand scale in Fig. 13 shows the applied osmotic stress in units of small calories. It is immediately clear that the pressures over which forces are observed correspond to perturbations that are less than thermal energy ($\approx$ 600 cal/mol) on most of the intervening water molecules.

McIntosh and coworkers have suggested from data on eggPC that there is an additional upward break in the pressure vs. spacing curve that is due to steric repulsion between bilayers that have less than approx. 10 water molecules per PC [107]. Such an upward break is not seen in the PC data processed as we have done here. Its appearance depends heavily on the definition of bilayer thickness. Should one expect interactions between hydrated polar species to be separable into hydration and steric components when the polar group conformations will always involve their associated water? Or does hydration repulsion combine both such interactions inasmuch as one expects continuously increased polar group restrictions from the very first steps of dehydration?

XIII. Hydration attraction?

In their review of structure in ordered phospholipid phases, Hauser [108] made clear the intricate pattern of hydrogen bonds among the phospholipid polar groups and their hydrating waters. These patterns are expected among phospholipids, such as certain PEs that take up relatively little water compared to PCs or to charged species [109,110]. Can the great strength of adhesion in these systems (Table I) be explained solely in terms of weakened hydration repulsion to allow a relatively strong van der Waals attraction? Or can solvent restructuring, thought to cause repulsion between hydrating surfaces, also mediate attraction between laterally ordered surfaces?

As noted above, multilayers of PE as a class tend to imbibe less water than PCs. Still, there is a larger range in the amount of uptake, natural PEs with heterogeneous chains, such as eggPE, swell the most. Remarkably even one methylation or the addition of methylated species to a bilayer will lead to sudden swelling of the multilayer lattice (Fig. 5). If one relies only on average properties of the bilayer surface, it is hard to see how a

generalized hydration repulsion and van der Waals force cause such different results with chemically similar surfaces.

However, the same Marcelja order-parameter formulation that describes hydration repulsion between like surfaces will also predict attraction between surfaces of opposite polarizing tendencies. Indeed, this formalism has been applied to the long-range attraction observed between DNA double helices. There, a characteristic 3 ångström exponentially decaying repulsion, much more cleanly defined than that seen among lipids, which becomes a 1.5 Å decay when DNA binds certain polyvalent cations. The shift in decay length is characteristic of the Marcelja model rederived for ordered heterogeneous surfaces.

We have suggested elsewhere [35] that the same kind of combined hydration repulsion and attraction might explain the shortened decay rate of repulsion between poorly swelling PEs such as POPE and that a solvent-structure-mediated attraction might explain the anomalously high attraction seen in these cases [36,52].

One should also be aware of a growing literature on attractive forces that will occur between surfaces of mutually orienting dipoles. Several models have recently appeared [112–114] using classical electrostatics to formulate a dipolar fluctuation force appropriate to polar zwitterions attached near a dielectric interface.

XIV. Conclusions

In a broad sense, any exertion to remove water is a form of hydration (or dehydration) force. One has grown accustomed to using 'hydration force' for that part of the exertion due to perturbation of water structure by the membrane or molecular surface. From this perspective it is puzzling why neutral bilayers will repel at an approx. 20 Å separation. But membrane undulation, polar group steric factors, electrostatic forces, and even van der Waals attraction might also contribute to the effort of dehydration. The real problem is to determine the distinguishing features, relative importance and interplay of these factors in what we have empirically called 'hydration forces'. A solution to the problem is impeded by many experimental uncertainties intrinsic to the structural disorder of most phospholipid liquid crystalline systems.

In phospholipid crystals where such disorder does not exist, X-ray crystallographic determinations show an intricate arrangement of polar groups with positive and negative charges neatly matched between facing bilayers, an intricate set of hydrogen bonds among lipid zwitterions and the few included water molecules (see, for example, Refs. 108 and 115). But most lipid species under most aqueous conditions do not form such dehydrated crystals. Apparently these precise arrangements of polar groups do not occur with such low energy as to create a significant driving force for crystal formation; a pre-existing order in the rest of the bilayer seems to be necessary. In fact most systems are driven to hydrate.

The simplest measure of hydration, maximum water uptake by neutral phospholipids, shows that disruptions of bilayer order – from double bonds in the hydrocarbon chain, from heterogeneity of chain type, from chain melting, from bulky methyl groups on polar amines – all seem to increase the uptake of water, to drive bilayers from crystalline arrangements. There is a kind of synergy in this drive. Disorder in the lipid causes water uptake by disrupted polar groups that concomitantly loosens bilayer structure. We find it remarkable that the equivalent molar concentration of zwitterions, even at full bilayer swelling, is far greater than the saturating solution concentration of these same polar groups existing as pure unattached solutes. But when they are attached to non-polar hydrocarbon chains, these closely packed polar groups virtually never precipitate into crystalline ordered arrays. The natural tension between the hydrophilic and hydrophobic parts keeps the polar groups themselves poised between precipitation and dissolution.

However, to go further, to describe the physical forces that swell the space between bilayers, one must rely heavily on definitions of bilayer thickness and separation. Difficulties are especially severe at low levels of hydration. Just as there is no mathematically ideal interface to define the progressive change from lipid to water regions, so there is no way to state boundaries without some idealization or ancillary construction. The progressive work of hydration, a pressure times a change in volume, is thermodynamically well-defined. Molecular dimensions are not. Different definitions – constructions based on very low resolution electron density maps with additional assumptions from models, or definitions based primarily on the water to lipid mass – lead to different comparative hydration strengths and even different features of the pressure vs. distance curves.

One such qualitative difference in feature has evoked the proposal of molecular steric interactions of polar groups. These are suggested by an upward break in the pressure vs. separation at less than 10 ångströms separation. But such a break is far more evident from low resolution electron density construction than from a mass average construction which so far suggests hardly any break at all. Clearly this region of high osmotic stress and very limited hydration merits far more study using both forms of data analysis. If this thermodynamic-structural work could be coupled with better probes of changes in polar group order – by neutron diffraction or by nuclear magnetic resonance, or perhaps by more precise analysis of thermal transitions – then the action of polar group steric forces would be more systematically understood.

At greater separations between bilayers, where polar group crowding between bilayers is no longer expected, there is still a question of how much of the observed hydration repulsion is due to straight affinity of water for the polar interface and to what extent that underlying force is enhanced by forces of membrane undulation. If means could be devised to monitor membrane disorder, as has been possible for forces between polyelectrolytes, then one would have a clearer idea of the magnitude of the underlying hydration itself.

In any event, there are questions about the molecular basis of hydration, about the mechanism by which water will be perturbed some layers from the surface. And of all the possible contributions to total hydration – do differences in total water uptake reflect differences in mechanisms of attraction between different kinds of polar layers? Or are there simply differences in strengths of repulsion with broadly similar van der Waals attractive forces? Does the presence of a net electrostatic charge that can drive bilayers to indefinitely large separation also affect surface-bound water to change surface hydration forces? Does the exclusion of solutes (small sugars or large polymers) that are unable to compete for water near the bilayer interface create thermodynamically different conditions for bilayer stability?

XV. Appendix

XV-A. Measuring bilayer thickness and separation

We describe the steps in determining bilayer thickness and separation and, from osmotic stress, the interbilayer force.

(1) Fig. 16 shows an example of the relation between the experimentally measured X-ray repeat spacing of the spontaneously formed multilammelar structure, d, and the weight percent lipid, c, in the samples determined by gravimetrically adding water to SOPC.

(2) On the basis of the densities of lipid and of water, c can be converted to the volume of water per lipid molecule V_w, the volume fraction of lipid in the same θ, and the area A available per lipid molecule on one plane perpendicular to the axis of the lamellar repeat.

$$\theta = 1/(1+(1-c)\cdot\nu_w/c\cdot\nu_l)$$

$$A = 2\cdot 10^{24}\cdot M\cdot\nu_l/\theta\cdot d\cdot N_0$$

$$V_w = (1-\theta)\cdot A\cdot d/2$$

MW_l is the molecular weight of the lipid, N_0 is Avogadro's number and ν_l and ν_w are the partial specific volumes of water and phospholipid, respectively.

These structural parameters are independent of the distribution of the water and lipid within the lamellar repeat distance d, i.e., are model independent. They are dependent, however, on a good knowledge of the partial specific volumes of the lipid. We have listed in Table IV the values used for the indicated lipids. These are taken from, and are consistent with the measurements and derivations from a number of references listed in Table IV).

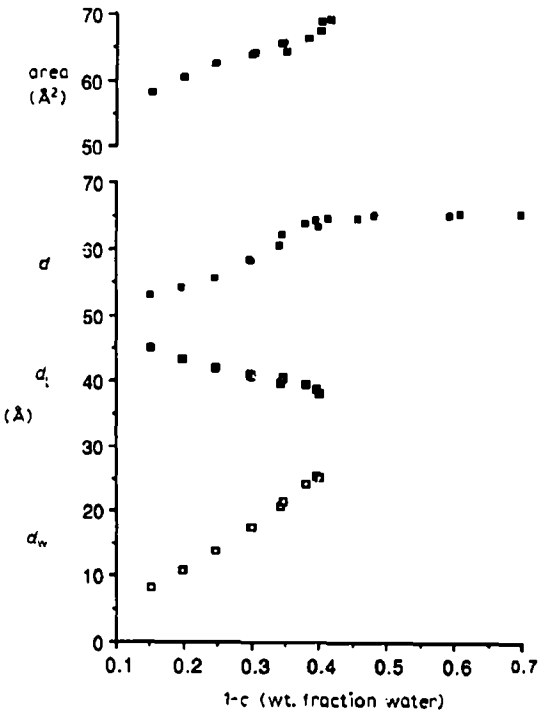

Fig. 16. Structural parameters of the lamellar phase formed by SOPC as they vary with water content and determined by X-ray diffraction. (■) d, lamellar repeat spacing; (□) d_l, bilayer thickness determined gravimetrically; (□) d_w, bilayer separation; (■) area available per molecule on a plane perpendicular to the direction of lamellar repeat.

Interesting observations emerge from these data.

(a) ν_l for CH_2 chains in bilayers are 1.05 cm^3/g if frozen and 1.17 if melted, and for hydrocarbon solutions are 1.07 and 1.29, respectively. This suggests that when constrained to bilayers the melted hydrocarbon chains have a lower partial volume than when free in solution.

(b) The lower value for melted chains in bilayers is required to give sensible polar group partial volumes. For example, from the measured value for DAG, 1.07, if $\nu_{hc} = 1.17$, $\nu_{pol} = 0.745$, comparable to the published value of 0.793 for glycerol. This correlation also requires that the C=O groups to be included in the polar group molecular weight.

(c) White et al. [73] have shown that the global partial specific volume of phospholipids does not change over the range of dehydration used to study interbilayer

TABLE IV

Partial specific volumes for lipids and their parts (cm^3/g) (Refs. in brackets)

Liquid paraffin	1.29 [116,118]
Melted hc	1.17 [117]
Melted hc, PC, PE	1.17 [117]
Crystalline hc	0.998 [117], 1.07 [118]
Crystalline hc PC	1.05 [118], 1.008, 1.006
Gly-Pc + C = O	0.668 [117], 0.758 [122], 0.713 DOPC, 0.768 DPPCm, 0.751 DPPCf
Serine-P	0.660 [119]
2-Amino-eth PO_4	0.640 [120]
Glycerol	0.793 [116] 0.745 DAG,
Gly-PE	0.693 [116] 0.67 DMPE, [116]
DPPC, DMPC, DSPC (gel)	0.94 [117]
DPPC (45° C)	1.005 [117]
DMPC (30° C)	0.98 [117]
DSCP (55° C)	1.02 [117]
DOPC (20° C)	0.990
DMPE	0.96 [121]
DAG	1.07
Synthetic PEs	0.96–1.02 [34]

forces. This lends credence to the structural parameters and their changes derived using the Luzzati formalism.

Table V provides molecular weights, partial volumes and compressibilities used to calculate the structural parameters of the lamellar phases of phospholipids.

(3) To proceed to define bilayer thickness and separation, assumptions are required about the distribution of water and lipid within the repeat distance d of the multilamellar phase. We describe three methods of doing this.

Using the Luzzati method, which assumes that the lipid and water pack into completely separate layers containing all and only the single component, d can be partitioned into a layer of lipid of thickness $d_l (= \theta \cdot d)$ and a layer of water of thickness $d_w (= d - d_l)$. Further, a knowledge of the molecular weights and densities of the hydrocarbon and polar parts of the lipid molecule (see Table V) allows the bilayer itself to be divided into hydrocarbon, $d_{hc} (= \theta_{hc} \cdot \theta \cdot d)$, and polar group layer, $d_p (= d_l - d_{hc})$, thicknesses where

$$\theta_{hc} = MW_{hc} \cdot \nu_{hc} / (MW_l \cdot \nu_l)$$

and MW_{hc} is the molecular weight of the hydrocarbon portion of the lipid molecule and ν_{hc} is the partial specific volume of that hydrocarbon.

Table VII provides the structural parameters and degrees of maximum hydration using this gravimetric method.

An alternative definition of bilayer thickness is used by McIntosh and Simon [27] and makes use of the electron density distribution of the bilayers, shown schematically in Fig. 3. To the peak-to-peak distance across bilayers, assumed to represent the distance between polar group phosphates or some fixed position near them, these authors add an estimated polar group thickness. These alternate approaches make a considerable difference in the way one estimates the distribution of water around the polar groups, and therefore of bilayer separation and definition of bilayer contact. Such differences are illustrated in Table VI for the fully hydrated lamellar phase and for the lamellar phase under moderate stress. The different definition of bilayer thickness leads naturally to the difference in absolute values of bilayer separation. However, what is striking is the opposite conclusion one obtains regarding the relative bilayer separations under moderate stress. McIntosh and Simon would conclude that gel DPPC bilayers are further apart than egg PC bilayers, we would conclude the opposite.

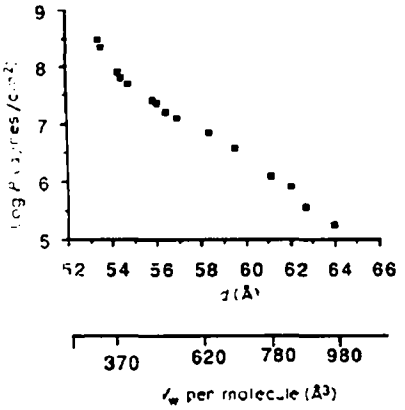

Fig. 17. Net interbilayer pressure, P, for SOPC, as it varies either with water content, V_w, the volume of water per lipid molecule or with lamellar repeat distance, d.

Each of these methods using X-ray dimensions suffers from too low a structural resolution to define bilayer thickness and separation adequately, and how, consequently, they change with dehydration. The latter is important in determining the hydration force parameters described below. Consequently, to determine the

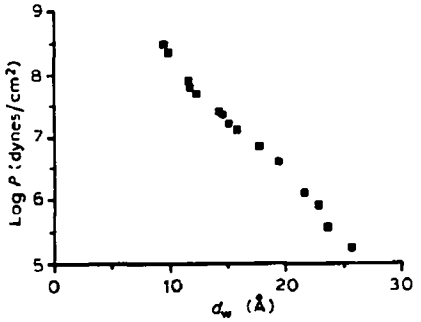

Fig. 18. Net interbilayer pressure, P, for SOPC, as it varies with interbilayer separation, d_w, determined gravimetrically.

TABLE V

Molecular weights of the total lipid (MW), its hydrocarbon (MW_{hc}) and of polar (MW_p) parts; lipid specific volume (ν, cm^3/g), and specific volume of the hydrocarbon part of the molecule (ν_{hc}); bilayer compressibility, K, and bilayer thickness, d_i, at the osmotic stress of log P = 7 used to calculate the structural parameters according to the formula described

	MW	MW_{hc}	MW_p	ν	ν_{hc}	K	d_i at log P = 7
DHDAA							
POPE	712	433	269	1	1.17	233	42.0 at 7.04
DOPS	832	471	361	1	1.17		
SOPC	786	475	311	1	1.17	200	41.2 at 7.08
DGDAG	933	462	471	1	1.17	200	39.1
POPE/SOPC							
9/1	715	444	271	1	1.17		
9/1	719	446	273	1	1.17	233	42.0 at 7.06
4/1	729	449	277	1	1.17		
2/1	731	454	277	1	1.17	222	41.9 at 7.03
3/2	741	455	286	1	1.17		
1/1	749	459	290	1	1.17		
DGDAG/SOPC 45/55	852	469	384	1	1.17	200	39.3 at 7.06
DGDAG/POPE 1/1	822	452	370	1	1.17	216	39.2 at 7.05
DOPE/DOPC 3/1	750	471	279	0.99	1.17	200	39
egg PE	733	464	269	1	1.17	200	34.1 at 7.01
Egg PEt	733	464	269	1	1.17	200	37.7
Egg PEt-Me	747	464	283	1	1.17	200	41.3 at 7.03
Egg PEt-Me_2	761	464	297	1	1.17	200	40.8 at 6.99
Egg PC	775	464	311	1	1.17	145	37.7 at 7.03
PC 16-22	800	490	310	1	1.17	145	39
Egg PC/Chol 1/1	1177	851	326	1.03	1.12	1000	42.1
DPPC/Chol 1/1	1120	810	310	1.02	1.12	600	43.3
Egg PC/DAG-12.5	787	455	332	1	1.17	145	37.3
DLPC	621	311	310	0.98	1.17	145	32.2
DMPC-27	677	367	310	0.98	1.17	145	36.4
DPPC-50	733	423	310	1.005	1.17	145	36.7
DOPC	787	471	316	0.99	1.17	145	36.6
DPPC-25	733	423	310	0.94	1.05	1000	47.2
DSPC	789	473	316	0.94	1.05	1000	47.8
DPPC/Chol 8/1	772	462	310	0.94	1.05	1000	50.9

changes in lamellar phase dimensions, the independently measured bilayer compressibility modulus, K [18], should be applied to the bilayer thicknesses measured by X-ray diffraction. This is illustrated for the gravimetric data using the following procedure, but it could just as well be applied to the dimensions derived using electron density profiles.

(4) Fig. 17 shows the experimentally determined relation between the net interbilayer pressure, P, and the repeat spacing, d, of the resultant lamellar phase, again for SOPC. The linear part of the curve can be described by

$$P = P_0 \exp(-d/\lambda_d)$$

By reference to the gravimetric data the repeat spacing, d, can be translated into the volume of water per lipid molecule and the relation between P and V_w (also shown in Fig. 17) can described by

$$P = P_0 \exp(-V_w/\mu)$$

By reference to the gravimetric data the repeat spacing, d, can also be partitioned as described above and again the linear part of the curve described by

$$P = P_0 \exp(-d_w/\lambda_{d_w})$$

The parameters for these three experimentally determined exponentials for many lipids are shown in Table VIII.

(5) The structural parameters d_i and d_w for the osmotic stress data which make use of the independently measured compressibility of the bilayers have then been derived in the following way. First, the bi-

TABLE VI

	at log $P = 0$			at log $P = 7$		
	d	d_1	d_w	d	d_1	d_w
Egg PC						
M and S [a]	63.2	47.8	15.4	56	49.5	6.5
R and P [b]	61.9	37	24.9	56	38.5	17.5
DPPC						
M and S	63.3	51.9	11.7	60.5	52	8.5
R and P	63.8	47.1	16.7	60.5	48	12.5

M and S, McIntosh and Simon; R and P, Rand and Parsegian.

layer thickness, d_1^* at log $P^* = 7$ is chosen, since the water content is known accurately and the compressibility of the bilayer, K, is in the linear range. Second, the compressibility modulus, K dyne/cm, measured by Evans and Needham [18] is used to calculate bilayer thickness, d_1, and separation, $d_w = d - d_1$, for all the osmotic stress experimental points where log $P < 8$. The actual values of d_1^* and K used for a variety of lipids are shown in Table V.

K is the fractional change in area for a change in bilayer tension, $\bar{T}$, and is equal to $\Delta\bar{T}/\Delta A/A_0$.

TABLE VII

Structural parameters of the fully hydrated lamellar phases as defined in this appendix and determined gravimetrically

	d_0 (Å)	c_0	A_0 (Å^2)	d_{ho} (Å)	d_{wo} (Å)	d_{ho} (Å)	d_{go} (Å)	V_{wo} (Å^3)	V_{wo}/PE (Å^3)
DDPE	45.8	0.72	55	32.5	13.3			365	365
DAPE	57.3	0.79	58	47.3	10			290	290
DLPE	46.1								270
POPE	53.2	0.78	56	41.3	11.7	30.1	11.2	328	328
DOPS	53.5	0.74	70	39.6	13.9	26.2	13.4	485	361
SOPC	64.4	0.60	66	39	26	27.6	11.4	858	742
DGDG	53.2	0.73	80	38.6	14.6	22.4	16.2	586	335
POPE/SOPC									
9/1	54.5	0.76	58	41.2	13.3	29.9	11.3	383	380
9/1	56.4	0.73	58	41.2	15.2	29.9	11.3	441	435
4/1	59.9	0.69	58	41.3	18.6	29.8	11.5	543	527
2/1	61.2	0.68	59	41.3	19.9	30.0	11.3	585	568
3/2	63.3	0.65	60	41.1	22.2	29.5	11.6	665	625
1/1	63.8	0.64	61	40.8	23	29.3	11.5	702	651
DOPE	52	0.70	65	37	15			487	487
DOPE-Me	61	0.63	62	39	22			682	648
DOPE-Me$_2$	62	0.60	66	38	25			825	747
DOPC	61	0.59	70	36	24			840	727
DGDAG/SOPC									
45/55	57.2	0.68	73	38.9	18.3	25.1	13.8	665	466
DGDAG/POPE									
1/1	54	0.72	70	38.9	15.1	25.0	13.9	530	385
DOPE/DOPC									
3/1	58	0.65	66	37.7	20.3	28.0	9.7	671	647
Egg PE	52.9	0.61	75	32.3	20.5	23.9	8.4	766	766
Egg PEt	52	0.70	66	36.5	15.5	27.0	9.5	517	517
Egg PEt-Me	61.8	0.60	67	37.1	24.7	27.0	10.1	827	786
Egg PEt-Me$_2$	63.1	0.58	70	36.3	26.8	25.9	10.4	938	850
Egg PC	61.9	0.57	74	35.1	26.8	24.6	10.5	992	858
PC 16-22	63.5	0.59	71	37.5	26	26.9	10.6	920	798
Egg PC/Chol 1/1	65.5	0.62	96	40.3	25.2	31.7	8.6	1210	998
DPPC/Chol 1/1	66	0.57	97	37.7	28.3	29.9	7.8	1365	1184
Egg PC/DAG-12.5	63	0.54	87	34.2	28.8	24.1	10.1	1253	971
DLPC	59	0.51	69	30	29	17.9	12.1	996	864
DMPC-27	62.2	0.56	65	34.5	27.7	22.3	12.2	903	784
DPPC-50	67	0.51	71	34.2	32.8	23.0	11.2	1168	1014
DOPC	64	0.50	82	32	32	22.6	9.4	1312	1117
DPPC-25	63.8	0.69	52	44.2	19.6	28.5	15.7	513	445
DSPC	67.3	0.68	55	45.5	21.8	30.5	15.0	596	507
DPPC/Chol 8/1	80	0.56	54	45	35	30.1	14.9	945	820

TABLE VIII

Exponential hydration force parameters describing the bilayer repulsive force using (a) log P vs. d, (b) log P vs. V_w, (c) log P vs. d_w gravimetric and (d) log P vs. d_w compressibility adjusted

Lipid	Grav. (d)		Grav. (vol)		Grav. (d_w)		Comp. (d_w)	
	λ_d	log P_0	μ	log P_0	λ_{dw}	log P_0	λ_c	log P_0
POPE	0.64	12.64	24.9	12.05	0.84	12.37	0.82	12.49
DOPS								
SOPC	1.55	23.19	81.9	9.8	2.29	10.14	1.98	10.51
DGDG	1.38	23.35	73.6	10.03	1.76	10.13	1.67	10.27
POPE/SOPC								
19/1								
9/1	0.94	32.12	36.8	11.04	1.24	11.24	1.26	11.16
4/1								
2/1	1.6	22.29	65.8	9.84	2.09	10.06	2.08	10.03
3/2								
1/1								
DGDG/SOPC 45/55	1.36	24.46	68.9	10.54	1.81	10.72	1.84	10.6
DGDG/POPE 1/1	1.25	25.23	61.1	10.33	1.64	10.55	1.72	10.3
DOPE/DOPC 3/1	1.48	22.36	70	9.56	2.09	9.75	1.78	10.19
egg PE	0.73	37.26	85.1	10.09	2.06	10.58	1.32	12.45
egg PEt	0.68	39.41	78.9	9.24	2.08	9.65	1.08	12.3
egg PEt-Me	1.36	24.48	78.9	9.21	2.33	9.46	1.76	10.28
egg PEt-Me_2	1.47	23.35	85.1	9.33	2.38	9.65	1.83	10.36
egg PC (RP) [a]	1.4	24.15	98.6	9.51	2.65	9.76	2.07	10.58
(MS) [b]							2.0	
PC 16-22	1.74	20.58	98.6	9.27	2.53	9.58	2.1	10.09
egg PC/Chol 1/1	1.07	30.94	72.3	11.97	1.40	12.6	1.08	13.8
DPPC/Chol 1/1	1.45	24.83	180.8	8.72	3.20	9.19	1.53	11.54
egg PC/DAG-12.5	1.87	20	160.7	9.18	3.17	9.62	2.37	10.37
DLPC	1.6	20.4	96.4	9.36	2.60	9.72	2.04	10.56
DMPC-27	1.96	18.92	90.4	9.52	2.60	9.94	2.16	10.49
DPPC-50	1.98	19.4	103.3	9.78	2.55	10.38	2.13	11
DOPC	1.63	21.61	120.6	9.25	2.90	9.6	2.11	10.63
DPPC-25 (RP)	1.04	32.3	53.6	9.63	2.00	9.83	1.07	12.3
(MS)							1.4	
DSPC	1.19	30.67	66.8	9.79	2.29	10.17	1.26	12.93
DPPC/Chol 8/1	1.98	21.93	88.6	8.9	3.00	9.47	2	10.74

[a] Values calculated according to the method of Rand and Parsegian.
[b] Values calculated according to the method of McIntosh and Simon.

For osmotic stress, changes from P^* to P cause changes in lateral tension $\Delta\bar{T} = (P - P^*) \cdot d_w$. The fractional change in area $\Delta A/A_0 = -\Delta d_l/d_l^* = (d_l^* - d_l)/d_l^*$ for constant lipid molecular volume. Hence $d_l/d_l^* = 1 + (P - P^*/K) \cdot d_w$ and, since $d = d_l + d_w$ then $d_l/d_l^* = (K + (P - P^*) \cdot d)/(K + (P - P^*) \cdot d_l^*)$ from which can be derived from the new d and P, the new d_l and other structural parameters.

We have shown that the derived parameters are independent of the chosen osmotic pressure for log P^* < 7.5.

Fig. 18 shows the relation between log P and d_w derived this way. As a descriptor of the data, the linear part of the log P vs d_w curves is then best fitted to $P = P_0 \exp(-d_w/\lambda_c)$. These are shown in Table VIII for a number of lipid species.

By extrapolating to low stress, the limiting value of d_l, and, therefrom, all the structural parameters describing the lamellar phase in excess water, can be determined. They are within error of the gravimetrically derived data. Since they come from the preferred method for deriving lamellar phase dimensions and hydration force parameters, these results are shown in Table II.

Acknowledgements

One of the unexpected pleasures of working on this subject is our interaction with many people who have now become drawn to it and whose studies figured so strongly in the work cited here. We would especially like to thank the following for their help and comments while preparing this review; Gregor Cevc, Sol Gruner,

Roger Horn, Tom McIntosh, Sid Simon and Gordon Tiddy. This work could not have been done without the expert support of Nola Fuller and the financial backing, for R.P.R., of the Natural Sciences and Engineering Research Council of Canada.

References

1 Clunie, J.S., Goodman, J.F. and Symons, P.C. (1967) Nature 216, 1203–1204.
2 Churaev, N.V. and Derjaguin, B.V. (1985) J. Coll. Interf. Sci. 103, 542–553.
3 Barclay, L.M. and Ottewill, R.H. (1970) Spec. Discuss. Faraday Soc. 1, 138–147.
4 Derjaguin, B.V. and Churaev, N.V. (1986) in Fluid Interfacial Phenomena (Croxton, C.A., ed.), pp. 663–738, John Wiley & Sons, Chichester.
5 Derjaguin, B.V., Churaev, N.V. and Miller, V.M. (1987) Surface Forces, Consultants Bureau, New York.
6 Luzzati, V. and Husson, F. (1962) J. Cell. Biol. 12, 207–219.
7 Small, D.M. and Bourges, M. (1966) Mol. Crystals 1, 541–561.
8 Parsegian, V.A. (1967) J. Theor. Biol. 15, 70–74.
9 LeNeveu, D.M., Rand, R.P. and Parsegian, V.A. (1976) Nature 259, 601–603.
10 LeNeveu, D.M., Rand, R.P., Parsegian, V.A. and Gingell, D. (1977) Biophys. J. 18, 209–230.
11 Parsegian, V.A., Fuller, N.L. and Rand, R.P. (1979) Proc. Natl. Acad. Sci. USA 76, 2750–2754.
12 Parsegian, V.A., Rand, R.P., Fuller, N.L. and Rau, D.C. (1986) Methods Enzymol. 127, 400–416.
13 Israelachvili, J.N. and Adams, G.E. (1978) J. Chem. Soc. Faraday Trans 1, 74, 975–1001.
14 Israelachvili, J. and Marra, J. (1986) Methods Enzymol. 127, 353–360.
15 Kwok, R. and Evans, E. (1981) Biophys. J. 35, 637–652.
16 Evans, E.A. (1980) Biophys. J. 31, 425–432.
17 Evans, E. and Metcalfe, M. (1984) Biophys. J. 46, 423–425.
18 Evans, E. and Needham, D. (1937) J. Phys. Chem. 91, 4219–4228.
19 Gruner, S.M., Parsegian, V.A. and Rand, R.P. (1986) Discuss. Chem. Soc. 81, 29–37.
20 Evans, E.A. and Needham, D. (1987) in Physics of Amphiphil layers (Meunier, J., Langevin, D. and Boccara, N., eds.), pp. 178–198, Springer-Verlag, Berlin.
21 Evans, E. and Kwok, R. (1982) Biochemistry 21, 4874–4879.
22 Evans, E. and Needham, D. (1986) Faraday Discuss. Chem. Soc. 81, 267–280.
23 Luzzati, V. (1968) in Biological Membranes (Chapman, D., ed.), pp. 71–123, Academic Press, New York.
24 Evans, E.A. and Skalak, R. (1980) in Mechanics and Thermodynamics of Biomembranes. CRC Press, Boca Raton.
25 Janiak, M.J., Small, D.M. and Shipley, G.G. (1979) J. Biol. Chem. 254, 6068–6078.
26 Lewis, B.A. and Engelman, D.M. (1983) Mol. Biol. 166, 211–217.
27 McIntosh, T.J. and Simon, S.A. (1986) Biochemistry 25, 4058–4066.
28 Horn, R. (1984) Biochim. Biophys. Acta 778, 224–228.
29 Marra, J. (1985) J. Coll. Interf. Sci. 107, 446–458.
30 Derjaguin, B.V. (1934) Kolloid-Z. 69, 155.
31 Marra, J. (1986) Biophys. J. 50, 815–825.
32 Horn, R.G., Israelachvili, J.N., Marra, J., Parsegian, V.A. and Rand, R.P. (1988) Biophys. J. 54, 1185–1187.
33 Rand, R.P. (1981) Annu. Rev. Biophys. Bioeng. 10, 277–314.
34 Seddon, J.M., Cevc, G., Kaye, R.D. and Marsh, D. (1984) Biochemistry 23, 2634–2644.
35 Seddon, J.M., Harlos, K. and Marsh, D. (1983) J. Biol. Chem. 258, 3850–3854.
36 Rand, R.P., Fuller, N.L., Parsegian, V.A. and Rau, D.C. (1989) Biochemistry, in press.
37 Ref. deleted.
38 Lis, L.J., McAlister, M., Fuller, N.L., Rand, R.P. and Parsegian, V.A. (1982) Biophys. J. 37, 657–666.
39 Gruner, S.M., Tate, M.W., Kirk, G.L., So, P.T.C., Turner, D.C., Keane, D.T., Tilcock, C.P.S. and Cullis, P.R. (1988) Biochemistry 27, 2853–2866.
40 Cevc, G. (1988) Ber Bunsenjesellschaft Phys. Chem., in press.
41 Jendrasiak, G.L. and Mendible, J.C. (1976) Biochim. Biophys. Acta 424, 149–158.
42 Das, S. and Rand, R.P. (1986) Biochemistry 25, 2882–2889.
43 Rand, R.P., Parsegian, V.A., Henry, J.A.C., Lis, L.J. and McAlister, M. (1980) Can. J. Biochem. 58, 959–968.
44 McIntosh, T.J., Magid, A.D. and Simon, S.A. (1988) Biochemistry 28, 17–25.
45 Rand, R.P. and Luzzati, V. (1968) Biophys. J. 8, 125–137.
46 Vaughan, D.J. and Keough, K.M. (1974) FEBS Lett. 47, 158–161.
47 Mulukutla, S. and Shipley, G.G. (1984) Biochemistry 23, 2514–2519.
48 Guldbrand, L., Jonsson, B. and Wennerstrom, H. (1982) J. Coll. Int. Sci. 89, 532–541.
49 Goldstein, R.E. and Leibler, (1988) S. Phys. Rev. Lett. 16, 2113–216.
50 Cevc, G. and Marsh, D. (1985) Biophys. J. 47, 21–31.
51 Cevc, G., Seddon, J.M. and Marsh, D. (1986) Discuss. Chem. Soc. 81, 179–189.
52 Marra, J. and Israelachvili, J.N. (1985) Biochemistry 24, 4608–4618.
53 Marra, J. (1988) J. Coll. Interf. Sci. 109, 11–20.
54 Cowley, A.C., Fuller, N.L., Rand, R.P. and Parsegian, V.A. (1978) Biochemistry 17, 3163–3168.
55 Loosley-Millman, M.E., Rand, R.P. and Parsegian, V.A. (1982) Biophys. J. 40, 221–232.
56 Pashley, R.M., McGuiggan, P.M., Ninham, B.W., Brady, J. and Evans, D.F. (1986) J. Phys. Chem. 90, 1637–1642.
57 Portis, A., Newton, C., Pangborn, W. and Papahadjopoulous, D. (1979) Biochemistry 18, 780–790.
58 Feigenson, G.W. (1986) Biochemistry 25, 5819–5825.
59 Florine, K.I. and Feigenson, G.W. (1987) Biochemistry 26, 1757–1768.
60 Eisenberg, M., Gresalfi, T., Riccio, T. and McLaughlin, S. (1979) Biochemistry 18, 5213–5223.
61 Parsegian, V.A. and Rand, R.P. (1983) Ann. N.Y. Acad. Sci. 416, 1–12.
62 Guldbrand, L., Jonsson, B., Wennerstrom, H. and Linse, P. (1984) J. Chem. Phys. 80, 2221–2228.
63 Kjellander, B. and Marcelja, S. (1985) Chem. Scripta 25, 112–116.
64 Helfrich, W. (1978) Z. Naturforsch. 33a, 305–315.
65 Sornette, D. and Ostrowsky, N. (1985) J. Chem. Phys. 45, 265.
66 Evans, E. and Parsegian, V.A. (1989) Proc. Natl. Acad. Sci. 83, 7132–7136.
67 Safinya, C.R., Roux, D., Smith, G.S., Sinha, S.K., Dimon, P., Clark, N.A. and Bellocq, A.M. (1986) Phys. Rev. Lett. 57, 2718–2721.
68 Podgornik, R., Rau, D.C. and Parsegian, V.A. (1988) Macromolecules 22, 1780–1786.
69 Carvell, M., Hall, D.G., Lyle, I.G. and Tiddy, G.J. (1986) Faraday Discuss. Chem. Soc. 81, 223–237.
70 Adam, C.G., Durrant, J.A., Lowry, M.R. and Tiddy, G.J.T. (1984) J. Chem. Soc. Faraday Trans. 1 80, 789–801.
71 Jendrasiak, G.L. and Hasty, J.H. (1974) Biochim. Biophys. Acta 337, 79–91.
72 Torbet, J. and Wilkins, M.H.F. (1976) J. Theor. Biol. 62, 447–458.

73 White, S.H., Jacobs, R.E. and King, G.I. (1987) Biophys. J. 52, 663–666.
74 Smith, G.S., Safinya, C.R., Roux, D. and Clark, N. (1987) Mol. Crystals and Liquid Crystals 144, 235–255.
75 Barouch, E.,Matijevic, E. and Parsegian, V.A. (1986) J. Chem. Society 82, 2801–2809.
76 Evans, E.A. and Parsegian, V.A. (1983) Ann. N.Y. Acad. Sci. 416, 13–33.
77 Bradley, W.F., Grim, R.E. and Clark, G.L. (1937) Z. Krist. 97, 216.
78 Viani, B.E., Low, P.F. and Roth, C.B. (1982) J. Coll. Interf. Sci. 96, 229–244.
79 Israelachvili, J.N. (1987) Acc. Chem. Res. 20, 415–421.
80 Pashley, R.M. (1981) J. Coll. Interf. Sci. 80, 153–162.
81 Pashley, R.M. (1981) J. Coll. Interf. Sci. 83, 531.
82 Rau, D.C., Lee, B.K. and Parsegian, V.A. (1984) Proc. Natl. Acad. Sci. USA 81, 2621–2625.
83 Rau, D.C. and Parsegian, V.A. (1987) Biophys. J. 51, 503.
84 Evans, D.F. (1988) Langmuir 4, 3–12.
85 Evans, D.F. and Ninham, B.W. (1986) J. Phys. Chem. 90, 226.
86 Rand, R.P. and Parsegian, V.A. 91986) Annu. Rev. Physiol. 48, 201–212.
87 Parsegian, V.A. and Rand, R.P. (1989) in Cellular Membrane Fusion. (Wilschut, J. and Hoeckstra, D., eds.), Marcel Dekker, New York.
88 Rand, R.P., Fuller, N.L. and Lis, L.J. (1979) Nature 279, 258–260.
89 Israelachvili, J. and Pashley, R. (1982) Nature (London) 300, 341.
90 Christenson, H.K. and Claesson, P.M. 91988) Science 239, 390–392.
91 Afzal, S., Tesler, W.J., Blessing, S.K., Collins, S.K. and Lis, L.J. (1984) J. Coll. Int. Sci. 97, 303–307.
92 Marcelja, S. and Radic, N. (1976) Chem. Phys. Lett. 42, 129–130.
93 Gruen, D.W.R. and Marcelja, S. (1983) J. Chem. Soc. Trans. Faraday II 79, 211–223.
94 Gruen, D.W.J. and Marcelja, S. (1983) J. Chem. Soc. Trans. Faraday II 79, 225–242.
95 Kjellander, R. and Marcelja, S. (1985) Chem. Phys. Lett. 120, 393–396.
96 Schiby, D. and Ruckenstein, E. (1983) Chem. Phys. Lett. 95, 435–438.
97 Cevc, G., Podgornik, R. and Zeks, B. (1982) Chem. Phys. Lett. 91, 193–196.
98 Cevc, G. (1985) Chem. Scripta 25, 96–107.
99 Cevc, G. and Marsh, D. (1987) Phospholipid Bilayers: Physical Principles and Models. John Wiley and Sons, New York.
100 Cevc, G. (1989) J. Phys. (submitted).
101 Cevc, G. (1987) Biochemistry 26, 6305–6310.
102 Simon S.A., McIntosh, J. and Magid, A.D. (1988) J. Colloid Interface Sci. 126, 74–83.
103 Kornyshev, A.A. (1985) Chem. Scripta 25, 63–66.
104 Dzhavakhidze, P.G., Kornyshev, A.A. and Levadny, V.G. (1988) Il Nuovo Cimento 10, 627–652.
105 Atford, P. and Batchelor, M.T. (1988) Chem. Phys. Lett. 149, 206–211.
106 Jorgensen, W.L., Gao, J. and Ravinohan, C. (1985) J. Phys. Chem. 89, 3470–3473.
107 McIntosh, T.J., Magid, A.D. and Simon, S.A. (1988) Biochemistry 26, 7325–7332.
108 Hauser, H., Pasher, I., Pearson, R.H. and Sundell, S. (1981) Biochim. Biophys. Acta 650, 21–51.
109 Kolber, M.A. and Haynes, D.H. (1979) J.Membr. Biol. 48, 95–114.
110 McIntosh, T.J. and Simon, S.A. (1986) Biochemistry 25, 4948–4952.
111 Parsegian, V.A., Rand, R.P. and Rau, D.C. (1985) Chem. Scripta 25, 28–31.
112 Kjellander, R. (1984) J. Chem. Soc. Faraday Trans. II 80, 1323.
113 Podgornik, R. (1988) J. Chem. Soc. Faraday Trans. II 84, 611–631.
114 Attard, P., Mitchell, D.J. and Ninham, B. (1988) Biophys. J. 53, 457–460.
115 Small, D.M. (1986) The Physical Chemistry of Lipids. Handbook of Lipid Research. Plenum Press, New York.
116 Handbook of Physics and Chemistry (1967) 47, c75.
117 Nagle, J.F. and Wilkinson, D.A. (1978) Biophys. J. 23, 159–175.
118 Templin, P.R. (1956) Ind. Engineering Chem. 48, 154–161.
119 Putkey, E. and Sundaralingan, M. (1970) Acta. Cryst B. 26, 782–789.
120 Kraut, J. (1961) Acta Cryst. 14, 1146–1152.
121 Wilkinson, D.A. and Nagle, J.F. (1981) Biochemistry 20, 187–192.
122 Abrahamsson, S. and Pascher, I. (1966) Acta Cryst. 21, 79–87.